WEIZMANN INSTITUTE OF SCIENCE

Thesis for the degree
Master of Science

Submitted to the Scientific Council of the
Weizmann Institute of Science
Rehovot, Israel

עבודת גמר (תזה) לתואר
מוסמך למדעים

מוגשת למועצה המדעית של
מכון ויצמן למדע
רחובות, ישראל

By
Sebastián Duque Mesa

מאת
סבסטיאן דוקה מסה

חיפוש פיסיקה חדשה עם אטומי רידברג
Search for New Physics with Rydberg Atoms

Advisor:
Ofer Firstenberg

מנחה:
עופר פירסטנברג

January 2019

ינואר תשע"ח

Time comes into it.
Say it.   Say it.
The universe is made of stories,
not of atoms.

—*The Speed of Darkness*, Muriel Rukeyser.

WEIZMANN INSTITUTE OF SCIENCE

Abstract

Physics
Department of Complex Systems

Master of Science

Search for New Physics with Rydberg Atoms

by Sebastián DUQUE MESA

High-precision frequency measurements of atomic transitions can be used to probe physics beyond the Standard Model [1, 2] and are bounded only by the ability to calculate nuclear and electronic effects. Precise isotope-shift measurements of ground and low-lying atomic states depend heavily on a detailed description of the nuclear structure and are therefore very difficult to calculate theoretically. In contrast, Rydberg states (atomic states with high principal n and angular ℓ quantum numbers) are less affected by nuclear and electronic systematics than low lying atomic states, mainly due to the large orbital radius of the valance electron and its negligible overlap with the nucleus.

This suggest Rydberg atoms as a good platform for searches of new physics, such as light force mediators between neutrons in the nucleus and electrons, as they are potentially able to disentangle the new physics observable from the unknown nuclear effects. Here we develop a strategy to formulate a set of observables that are sensitive to the presence of new mass-dependent light mediators in Rydberg atoms and are independent to leading order of nuclear effects.

Acknowledgements

✉

Dear Sebastian,

I hope that you are already happily married. Congratulations.

I vaguely remember that when we met in Medellin you told me about your paper showing that light transfer in chlorophyll molecules [...]

Thanks, Uzy.

✉

Dear Uzy,

I am married already! Surprising, isn't it?

I understand Batel (now my wife) talked to you before we went to Cyprus.

Of all of the possible outcomes of me coming to Israel this is the one I would never had thought about. Crazy, isn't it?

Anyhow, whatever it was I will always blame it on you!

Now, regarding science: [...]

Best, Sebastián

Yes! I blame it on Uzy who, to show his appreciation on my hospitality when he was in Colombia, and instead of getting me a twenty dollars hard-copy of 2666 —the book of a Chilean writer he was happening to read at the time—, decided to speak in detail with Roee about my education, work and interest (well, I don't know how Uzy happened to know all of that).

Then on Roee, who listened to Uzy and brought me here. On Ofer that after that welcomed me to his group. On Ohr who patiently helped me to build a cavity when I had no experience. On Ran who supervised the progress on that cavity and my first visits to the desert (amazing!). On Gal and Lee for taking over my unfinished lab projects. On Ohad for those enlightening physics discussion we had over the homeworks. I blame it also on all of you!

In the middle of all that I met Arnaud and Rachel. They were, and I hope they will always be, ready to eat my baked salmon. Ah, and sorry Arnaud for not being able to spell your last name: that's why I will always keep calling you *Arnaud, my friend*.

Solitude, the longing for home, the long hours of silence at Clore's room. Well, there is a huge appreciation for those moments. They happened to be the foundation for the things yet to come.

Mis papás y mis hermanos—que me devolvieron a Israel cuando yo solo quería dejar todo atrás y quedarme allá, cómodo y protegido en el infinito amor de ellos.

David. Que ahí, siempre presente tras el teléfono, suele decir ¿has escuchado sobre el mito de Eros y Psique?

Batel, for you no words. For you all those things yet to come.

Contents

Chapter 1

Introduction

The Standard Model of particle physics (SM) successfully describes and predicts numerous phenomena up to the TeV scale, and it is theoretically consistent up to a much higher energy. However, the SM has major problems as it cannot account for other experimentally observed phenomena. For example, it has no dark matter particle that can explain observational measurements of gravitational interaction, it cannot explain the baryonic asymmetry or imbalance of matter anti-matter in the observable universe, nor it can predict neutrino oscillations. The above provides a strong motivation to look for new particles beyond those included in the SM. Although efforts concentrate in the search of New Physics (NP) in colliders and high-intensity experiments, optical tabletop experiments can also be used as new high-precision approaches to probe low-energy NP processes [1].

Such high-precision frequency measurements are bounded by the ability to calculate nuclear and electronic effects but do not rely on exact knowledge of the SM contributions to the atomic transitions [2]. Precise isotope-shift measurements of ground and low-lying atomic states depend heavily on a detailed description of the nuclear structure and are therefore very difficult to calculate. This measurements also require atomic systems with a number of stable isotopes which is uncommon [3]. In contrast, Rydberg states (atomic states with high principal n and angular ℓ quantum numbers) of Alkali-metal atoms or ionized Alkali earth metals are less affected by nuclear and electronic systematics than low lying atomic states, mainly due to the large orbital radius of the valance electron and its negligible overlap with the nucleus. This suggest Rydberg atoms as a good platform for searches of NP, such as low-mass force mediators between neutrons in the nucleus and electrons, as they are potentially able to disentangle the NP observable from the unknown nuclear effects and thus alleviate the need for a large number of isotopes.

In this thesis, a strategy is developed to formulate a set of observables that are sensitive to the presence of new mass-dependent NP force mediators in Rydberg atoms and are independent to leading order of nuclear effects, requiring as a consequence less isotopes than other approaches.

In §2 the non-relativistic atomic Hamiltonian and the effective model potential that describes the interaction of the Rydberg

electron with the charge distribution of the core electrons is introduced. §3 explains how the parameters of the model potential in a polarization plot, and the electronic and nuclear factors in a King's plot, can be extracted from experimental measurements. The appearance of a new force carrier, as described in §4, will lead to deviations from the predicted spectra allowing for atomic investigation of physics beyond the standard model. These investigations are then described in §5 in the context of Rydberg atoms, where advantages over other approaches are discussed. Finally in §6, the projected bounds on new physics are compared with other existing bounds. We conclude by discussing future directions.

El Modelo del Átomo

Con la taza de café caliente me enfrento a aquello que dejé escrito en la pantalla la noche anterior: *ecuación diferencial ordinaria no lineal no homogénea de segundo orden con condiciones en la frontera*. El modelo del átomo. Una sentencia. Tomo un sorbo de la taza con la esperanza que la fuerza de los granos molidos me ayude a enfrentar esa ecuación que sigue estando frente a mí. Ahí, en ese momento, soy extraño a mí mismo, soy yo en la frontera. ¿Cómo aprehender eso, esa ecuación, que no es realidad ni materia, tan intangible, tan silenciosamente secreta?

Todo, la materia y el átomo, la mezcla de elementos que en su inmutabilidad y eternidad dan origen a la realidad es imperceptible a los sentidos. Eternos, indivisibles, homogéneos, incomprensibles e invisibles. El racionamiento lógico de Demócrito me salva de la incomodidad que me ataca mientras estoy en esta silla, me protege del afán de desmontar el mecanismo interno del universo y entender su incomprensibilidad. Así como hay verdades pero no verdad debo aceptar que eso que está frente a mí, aquella ecuación, aquel átomo, no es posible entenderlo—no porque no pueda sino porque no se puede. El aroma del café, la tibieza de la taza y el sudor en mis manos mientras escribo en el papel, la temperatura gélida del aire acondicionado que lucha contra el verano afuera de mi ventana, el sonido del pájaro que grazna mientras la cruza, todo eso lo siento. Pero si lo siento todo, ¿cómo puedo explicarlo? ¿cómo relacionarme con un mundo que no entiendo y que no puedo desarmar, observar sus piezas y el vacío entre ellas para luego rearmar otra vez? ¿cómo negar el entendimiento de aquel mundo cuya fuerza experimento, negarme a mí mismo y a lo que me rodea? Seré siempre extraño a mí mismo.

Pasa el tiempo y el café se enfría, para desatarme de aquella ecuación que me oprime y me empuja contra la silla busco una imagen. Lentamente aquel átomo indivisible e invisible toma forma y aumenta su tamaño. Primero es un cubo, todos los componentes de aquel tan infinitamente punto sin estructura brotan y se redistribuyen en la geometría de los vértices, en las conexiones de las aristas. Mi esperanza aumenta, enumero sus propiedades y voy a confrontarlas con aquellas de la ecuación que persiste en la pantalla. No es suficiente, aún no se encuentran. Me libero de la rigidez del sólido platónico y el átomo se amplia, adquiere la textura abollonada y el sabor azucarado del pudín, sus componentes se esparcen como frutas en la superficie. En el calor, la forma y el sabor del pudín entiendo algo más y el secreto se comienza a revelar, veo entre los vericuetos de aquella formula la luz de la verdad. Pero, no es suficiente aún. Aquel pudín en su irregularidad encuentra a la vez su falsedad. Sin uniformidad no hay simetría. Persisto en la búsqueda y dibujo algo más dentro de mí. Nubes, órbitas, ondas. Un invisible sistema planetario, un universo abigarrado de extensión magnifica que se reduce al átomo, al electrón, al punto, a una imagen. Todo aquello lo veo, lo puedo experimentar y exacerba mis sentidos.

Sigue obstinado el texto en la pantalla, *ecuación diferencial ordinaria no lineal no homogénea de segundo orden con condiciones en la frontera*, pero ahora se cuela entre los márgenes de aquella fórmula el infinito, algo de lucidez. No naufrago en aquel pequeño universo que ensambla la realidad, en la experiencia de lo imperceptible, en la percepción de lo invisible. Navego entre imágenes y sensaciones. Sin embargo, esa sigue sin ser la realidad, son solo metáforas. Tomo el último sorbo de café, dejo la taza entre libros y papeles; ahí me esperará inmutable hasta mañana. Me levanto de la silla y en la pantalla persiste constante el mismo texto. Una sentencia. No es ciencia lo que hago, es pura poesía.

The Model of the Atom

With a cup of hot coffee, I am faced with that I left written on the screen the night before: non-linear non-homogeneous ordinary differential equation of second order with boundary conditions. The model of the atom. A sentence. I take a sip from the cup with the hope that the force of the dark grinded beans helps me deal with the equation in front of me. There, at that moment, I'm a stranger to myself, myself at the boundary. How to apprehend that, that equation, which is neither reality nor matter, so intangible, so silently secret?

All, the matter and the atom, the blend of elements that give rise to the reality in its immutability and eternity is imperceptible to the senses. Eternal, indivisible, homogeneous, incomprehensible and invisible. That, the logical reasoning from Democritus, saves me from the discomfort that takes over me while I sit in this chair, holds me back from disassembling the inner mechanism of the universe and understand its incomprehensibility. As long as there are truths but not Truth I must accept that the thing in front of me, the equation, that Atom, is impossible to understand—not because I cannot but because it cannot be. The aroma of the coffee, the warmth of the cup and the sweat in my hands while I write in the paper, the gelid temperature of the air-conditioning fighting against the stubborn summer outside the window, the sound of the quaking bird crossing the landscape, all that I sense. But if I feel all of that, how can I explain it? How would I relate to a world that I do not understand and that I cannot disassemble, that I cannot objectivize its parts and the voids in between them? How to refuse to the understanding of that world whose weight I experiment, to deny my self and everything around me? I'll always be a stranger to myself.

Time passes and the coffee cools, to get rid of what oppresses me and pushes me against the chair I look for an image. Slowly I imagine the components of the atom. A cube, the infinitive point without structure suddenly sprouts and redistribute in the geometry of vertices, in the connections of the edges of a solid. My hope increases, I enumerate its properties and I am going to confront them with those of the equation that persists on the screen. It is not enough, they do not match yet. I free myself from the rigidity of the Platonic solid and the atom expands, acquires the embossed texture and the sugary taste of a pudding, its components spread like fruits on the surface. In the heat, the shape and the taste of the pudding I understand something else about it and the secret begins to reveal, I see between the twists and turns of that formula some light. But, it's not enough yet. That pudding in its irregularity at the same time finds its falsity. Without uniformity there is no symmetry. I persist and try to draw anew in my imagination. Clouds, orbits, waves. An invisible planetary system, a variegated universe of magnificent extension that is reduced to the atom, to the electron, to the point, to an image, imagination. I see everything, I can experience it and it exacerbates my senses.

Yet the stubborn text stays still on the screen, non-linear non-homogeneous ordinary differential equation of second order with boundary conditions, but now a part of the infinity, something of lucidity, creeps between the margins of that formula. Not shipwrecked in that small universe that assembles reality, in the experience of the imperceptible, in the perception of the invisible, I browse between images and sensations. However, that is not reality yet, all these are only metaphors. I take the last sip of coffee, I leave the cup between books and papers; there it will wait unchanged for me until tomorrow. I get up from the chair and the same text persists on the screen. A sentence. It is not science what I am doing here, it is poetry.

Chapter 2

Revisiting the Atomic Model

In this section, we discuss the electronic level structure of alkali atoms and we present the non-hydrogenic effects coming from the appearance of inner-shell electrons and the lifting of the point-like nucleus approximation.

Let us start with the simplest quantum mechanical approach to describe the atomic level structure: Bohr's model. In there the atom is depicted as a small, infinitely massive, positively charged nucleus with Z protons orbited by an electron attracted by the electrostatic force. This model is a close description of the Hydrogenic atom with Z proton in the nucleus and a single valence electron, where the energy levels

$$E_n^{(\infty)} = -\frac{m_e}{2\hbar^2} \left(\frac{e^2}{4\pi\epsilon_0} \right)^2 \frac{Z^2}{n^2} = -(2\pi\hbar) R^{(\infty)} \frac{Z^2}{n^2} \qquad (2.1)$$

lead to the Rydberg series

$$\nu_{n\to n'}^{(\infty)} = R^{(\infty)} \left(\frac{Z^2}{n'^2} - \frac{Z^2}{n^2} \right). \qquad (2.2)$$

Here

$$R^{(\infty)} = \frac{m_e}{4\pi\hbar^3} \left(\frac{e^2}{4\pi\epsilon_0} \right)^2 = \frac{\alpha^2}{2\lambda_e} \qquad (2.3)$$

is the Rydberg's constant and the superscript (∞) stands for the infinitely massive nucleus approximation, α is the fine structure constant and λ_e the Compton wavelength of the electron.

This simple perspective of atomic levels breaks as soon as we move down on the periodic table into the alkali atoms. Alkali atoms have one electron in the outermost orbital (similar to the Hydrogen atom) but the presence of inner–shell electrons and the finite size and mass of the nucleus introduce complex effects that are not accounted for in the Hydrogenic model. Moreover, corrections coming from relativistic effects associated with the fine structure constant α must be taken into account. This effects are well known and lead in first order in $(Z\alpha)^2$ to the fine-structure features of the atom. On the other hand, at scales close to the Compton wavelength of the electron λ_e, quantum electro-dynamic corrections become important leading to a number of

effects like the Lamb shift of the levels.

For now we'll examine the non-Hydrogenic effects due to the inner-shell electrons and the lifting of the point-like nucleus approximation. To do so lets consider the non-relativistic Hamiltonian of an atom with N_c core electrons located at positions $\mathbf{x}_i$ (for $i = 1, \dots, N_c$) and one valence electron at $\mathbf{x}$, together with a nucleus of mass m_A at $\mathbf{x}_N$,

$$H = \frac{p_N^2}{2m_A} + \sum_{i=1}^{N_c} \frac{p_i^2}{2m_e} + \sum_{i=1}^{N_c} V_{eN}(\mathbf{x}_i - \mathbf{x}_0) + \frac{1}{2} \sum_{i \neq j}^{N_c} V_{ee}(\mathbf{x}_i - \mathbf{x}_j)$$
$$+ \left[\frac{p^2}{2m_e} + V_{eN}(\mathbf{x} - \mathbf{x}_0) + \sum_{i=1}^{N_c} V_{ee}(\mathbf{x}_i - \mathbf{x}) \right], \quad (2.4)$$

where $V_{eN}(\mathbf{x}_i - \mathbf{x}_0)$ is the Coulomb potential between i–th electron with the nucleus and $V_{ee}(\mathbf{x}_i - \mathbf{x}_j)$ the one between electrons. The dynamics are best described in the center of mass (CM) frame where the Hamiltonian reduces to[1]

$$H = \sum_{i=1}^{N_c} \left[\frac{1}{2\mu} p_i^2 + \frac{1}{m_A} \sum_{j \neq i}^{N_c} \mathbf{p}_i \cdot \mathbf{p}_j + V_{eN}(\mathbf{r}_i) + \frac{1}{2} \sum_{j \neq i}^{N_c} V_{ee}(\mathbf{r}_i - \mathbf{r}_j) \right]$$
$$+ \left[\left(\frac{1}{2\mu} p^2 + V_{eN}(\mathbf{r}) \right) + \frac{1}{2m_A} \sum_{i=1}^{N_c} \mathbf{p} \cdot \mathbf{p}_j + \sum_{i=1}^{N_c} V_{ee}(\mathbf{r}_i - \mathbf{r}_j) \right],$$
$$(2.5)$$

where $\mu^{-1} = m_A^{-1} + m_e^{-1}$ is the reduced mass of the atom [4, 5]. The suggestive separation of core and valence electron dynamics relies on the fact that the valence electron is distinguishable from the core electrons, an assumption that is true for Rydberg levels—highly excited levels of the valence electron.

From the Hamiltonian above we can observe two distinct mechanisms that contribute to the deviation from the Bohr model, equation (2.1). First, electronic effects are introduced by the Coulomb interactions between tightly bound electrons in the inner shell (usually inactive during single electronic transitions) and outer-core valence electrons that give rise to the energy structure of the system and chemical properties of the elements. Even more, multi-electron correlations will appear in the non-separability of the system's wavefunction. On the other hand, nuclear effects due to the appearance of nuclear structure will give rise to further deviations in the energy spectrum of the atom, and are known as Field Shift (FS). Other nuclear related effects due to the mass modification of the atom are encapsulated on the terms proportional to the nuclear mass m_A and the atomic reduced mass μ. Due to their mass dependence, these effects are known as Mass Shifts (MS).

To see how these come into play, let's take a look again at our atomic Hamiltonian (A.4). To see separately the contributions coming from the nucleus, the core electrons and the valence

electron it can be rewritten as

$$H = H_{\text{core}} + H_{\text{valence}} + V_{\text{int}} + V_{\text{nucleus}}, \qquad (2.6)$$

where the Hamiltonian of the valence electron

$$H_{\text{valence}} = \frac{p^2}{2\mu} - \frac{e^2}{4\pi\epsilon_0}\frac{1}{r} \qquad (2.7)$$

is taken to be Hydrogen-like and is the 0-th order Hamiltonian that will be used for perturbation theory. The multi-electron Hamiltonian

$$H_{\text{core}} = \sum_{i=1}^{N}\left[\frac{1}{2\mu}p_i^2 + \frac{1}{2m_A}\sum_{j\neq i}^{N_c}\mathbf{p}_i\cdot\mathbf{p}_j + V_{\text{eN}}(\mathbf{r}_i) + \frac{1}{2}\sum_{j\neq i}^{N_c}V_{\text{ee}}(\mathbf{r}_i - \mathbf{r}_j)\right] \qquad (2.8)$$

includes the effects of the presence of the electron shell, the isotopic potential

$$\begin{aligned}
V_{\text{nucleus}}(\mathbf{r}) &= \frac{e^2}{4\pi\epsilon_0}\frac{Z}{r} + V_{\text{eN}}(\mathbf{r}) \\
&= \frac{e^2}{4\pi\epsilon_0}\frac{Z}{r} + \frac{e}{4\pi\epsilon_0}\int d^3r'\,\frac{\sigma(\mathbf{r}')}{|\mathbf{r}'-\mathbf{r}|} \qquad (2.9)
\end{aligned}$$

accounts for the Isotope Shifts (IS) deviations due to nuclear effects, both the extended charge distribution of the nuclei $\sigma(\mathbf{r})$ and the Specific Mass Shifts (SMS) of the valence electron[2]. The last term,

$$V_{\text{int}}(\mathbf{r}) = \sum_{i=1}^{N_c}V_{\text{ee}}(\mathbf{r} - \mathbf{r}_i) \qquad (2.10)$$

includes the Coulomb interaction between the valence electron and the charge distribution of the shell electrons.

[2] Notice that the nuclear effects in the core electrons are included in the multi-electron Hamiltonian H_{core}. This implies that the core Hamiltonian is Isotope dependent.

2.1 Multi-electron Effects and the Effective Model Potential

In addition to the electron-nucleus interaction V_{eN} binding the electron to the atom there exists another interaction term V_{ee} appearing from the interaction between electrons. This many-body interaction between the Z electrons composing the atom renders the problem analytically intractable—meaning that we cannot solve exactly the Schrödinger equation for this Hamiltonian. Furthermore, the Hamiltonian above does not include relativistic corrections that are important and lead, for example, to the spin-orbit structure of the energy levels. This relativistic corrections are part of the future perspectives of this work.

However, as already suggested before, considering the valence electron to be distinguishable from the core electrons helps

to simplify the problem. As seen in equation (2.6), there are pieces of the Hamiltonian that act in the Hilbert subspace of the valence electron or in the core electrons subspace, whereas the interaction potential couples both subspaces. A good starting point is the product wavefunction

$$|\Psi_{\gamma,n\ell}\rangle = |\varphi_{\gamma}^{C}\rangle\,|\psi_{n\ell}\rangle \tag{2.11}$$

where φ_{γ}^{C} is the zeroth order wavefunction of the electronic core with quantum numbers γ and $\psi_{n\ell}$ the wavefunction of the valence electrons. The valence electron wavefunctions are the eigenstates of the Hamiltonian H_{valence}, this are no other than the known analytical eigenfunctions of the Hydrogenic atom

$$H_{\text{valence}}\,|\psi_{n\ell}\rangle = E_{n\ell}^{(\mu)}\,|\psi_{n\ell}\rangle \quad \text{with} \quad E_{n\ell}^{(\mu)} = -\frac{\mu}{2\hbar^2}\left(\frac{e^2}{4\pi\epsilon_0}\right)^2\frac{Z}{n^2}; \tag{2.12}$$

whereas the core states φ_{γ}^{C} and their eigenenergies E_{γ}^{C} are only known formally through a Hartree-Fock type calculation

$$H_{\text{core}}\,|\varphi_{\gamma}^{C}\rangle = E_{\gamma}^{C}\,|\varphi_{\gamma}^{C}\rangle. \tag{2.13}$$

2.1.1 Polarization effects

Using the approach described above, it is possible to study with a perturbation theory the valence electron interaction with the core in terms of the potential

$$V_{\text{int}}(\mathbf{r}) = -\frac{e^2}{4\pi\epsilon_0}\sum_{i=1}^{N_c}\frac{1}{|\mathbf{r}_i - \mathbf{r}|}. \tag{2.14}$$

In most of the cases, core electrons remain inactive during the optical transitions of our interest and it is assumed that the cores of the atomic species under study will have zero angular momentum[3]. Even more, Hartree-Fock theory predicts that the potential of closed subshells is spherically symmetric, such that the valence electron orbitals are solution to a central field problem [6, §7.4]. In fact, to second order in perturbation theory, a multipole expansion of the potential (2.14) will lead to energy shifts of the form

$$\Delta E = -\sum_{k=1}^{\infty}\frac{\alpha^{Ek}}{2}\,\langle\psi_{n\ell}|r^{-2(k+1)}|\psi_{n\ell}\rangle \tag{2.15}$$

where the coefficients

$$\alpha^{Ek} \equiv 2\sum_{\gamma'}\frac{\langle\varphi_{\gamma}^{C}|\sum_{i=1}^{N_c}r_i^k C^k(\hat{r}_i)|\varphi_{\gamma'}^{C}\rangle}{E_{C}^{(0)}(\gamma) - E_{C}^{(0)}(\gamma')} \tag{2.16}$$

are the multipole polarizabilities of the charge distribution of the core electrons. This approximation is good for valence electrons in high-ℓ angular momentum orbitals with no overlap with the

[3] For atoms with nonzero core angular momentum the first order perturbation energy in V_{int} gives a series of terms in the even permanent electric moments of the core, leading to tensor fine structure.

charge distribution of the core electrons[4]. Dominant contributions for this kind of states will come from dipole and quadrupole polarizabilities, the energies shifts will be predicted by the effective polarizability potential

$$V_{\text{pol}} = -\frac{1}{2}\frac{\alpha^{E1}}{r^4} - \frac{1}{2}\frac{\alpha^{E2}}{r^6} \tag{2.17}$$

where the expectation values is over the Hydrogenic wavefunctions of the valence electron[5].

To effectively include low-ℓ states with penetration to the core, one can weight the long range polarization effects with the cut-off functions $W_n \equiv 1 - e^{-x^n}$ that suppresses the short-range behavior as [11]

$$V_{\text{pol}}(r) \approx -\frac{\alpha^{E1}}{2r^4}W_6\left(\frac{r}{r_c}\right) - \frac{\alpha^{E2}}{2r^6}W_8\left(\frac{r}{r_c}\right) \tag{2.18}$$

where r_c is a phenomenological electronic core radius.

The scale of this polarization effect for different alkali species can be seen in the left panel of figure 2.2a. Notice how the effect is qualitatively similar in all the atoms but is weighted by the number of electrons in them. That is, as the number of core electrons increases, the size of the polarization effect is higher, because the Coulomb interaction between the core electrons and the valence electron increases, and as such the effective polarizabilities.

2.1.2 Screening

The assumption that the valence electron is distinguishable and nonpenetrating into the electronic core distribution, as expressed in equation (2.11), holds for sufficiently high-ℓ states. However in order to establish and set limits on possible contributions from core penetration and exchange, it is important to model these contributions. To see how, consider the case of an Alkali atom. In such a case the single valence electron will move in the electrostatic field of the nucleus produced by the Z protons, however this field will be screened by the $Z - 1$ inner electrons as depicted in figure 2.1.

Near the nucleus, the valence electron will experience the unscreened Coulomb potential $-Ze^2/4\pi\epsilon_0 r$ and, as we get far away of the nucleus, its charge will be completely screened to one unit $-e^2/4\pi\epsilon_0 r$.

In a multi-electronic self-consistent approach, calculations of the electronic core wavefunctions φ_γ^C are available, then one can construct the penetration potential from the known orbital wavefunctions of the core electrons shells as in Ref. [12].

[4] See §3.9 on Ref. [7] for a short introduction, or Refs. [8–10] for a very detailed calculation.

[5] For bookkeeping reasons, we shall use the naming convention $\alpha_d \equiv \alpha^{E1}$ for dipole polarizability and $\alpha_q \equiv \alpha^{E2}$ for the quadrupole polarizability.
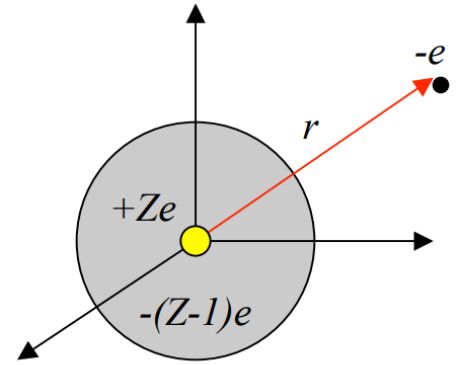

Figure 2.1: Shell model of the multi-electron Alkali atom: $Z - 1$ electrons screen the charge of the nucleus whereas only one electron that can penetrate this shell is actively involved in the atomic transitions.
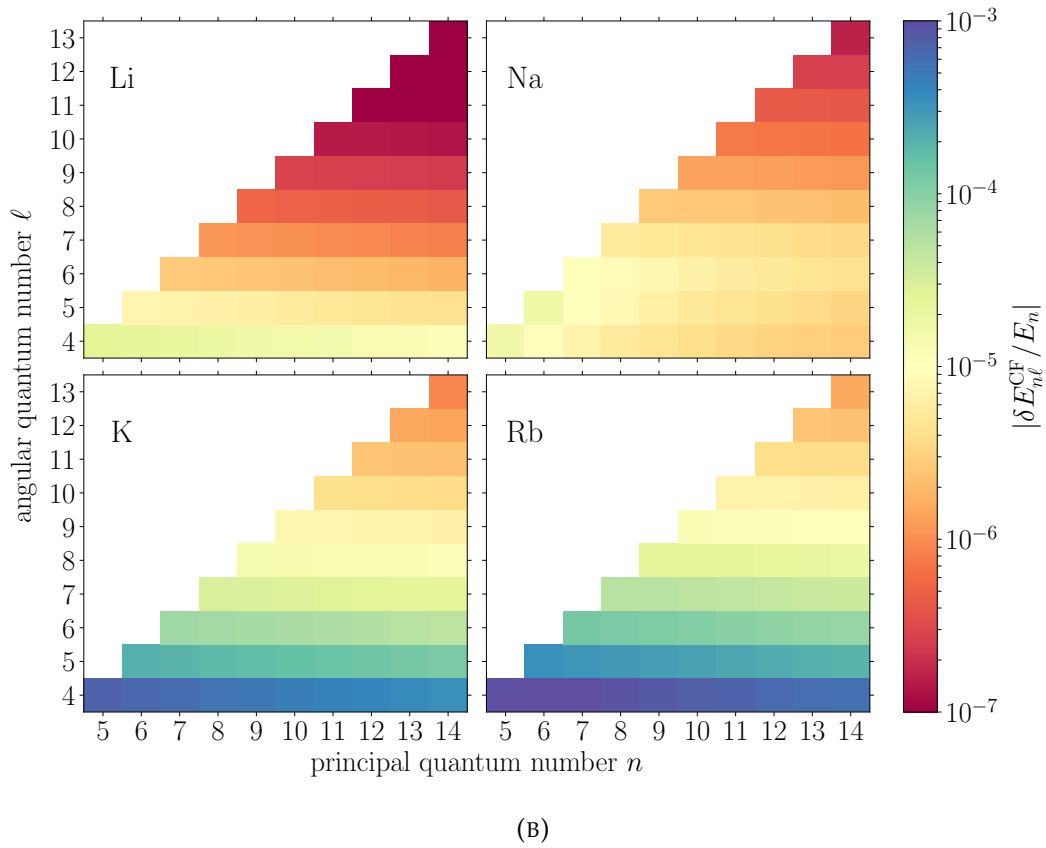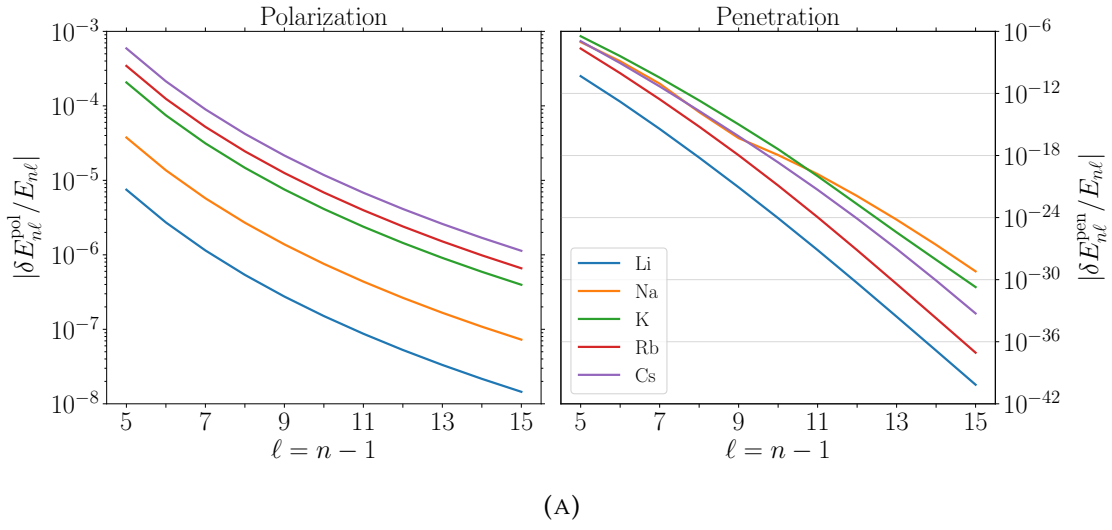
FIGURE 2.2: Size of the multi-electron effects with respect to the ionization energy $E_{n\ell}$ of the level (a) for circular states $\ell = n - 1$ in the alkali metal atoms labeled, notice the different scales on the plot for polarization (right side) and penetration (left side); and the total effect (b) for several $n\ell$ states of some alkali atoms.

However, generally such core wavefunctions are not available and then this approach becomes inconvenient and one needs to phenomenologically include penetration and exchange effects. To phenomenologically include electronic screening, one can use a position dependent nuclear charge in the electron-nucleus interaction potential in the valence electron Hamiltonian (2.7), such that effectively the coulomb potential $-Ze^2/4\pi\epsilon_0 r$ becomes

$$V_{\text{pen}}(r) = -\frac{1}{4\pi\epsilon_0} \frac{Z_{\text{eff}}(r)e^2}{r} \qquad (2.19)$$

in which

$$\lim_{r\to 0} Z_{\text{eff}}(r) = Z \quad \text{and} \quad \lim_{r\to\infty} Z_{\text{eff}}(r) = 1, \qquad (2.20)$$

as shown in figure 2.3.

In general the correction to the nuclear charge will be dictated by the radial probability distribution of the valence electron—the probability of finding the valence electron inside the core. The phenomenological position-dependent weight function that interpolates the value of the charge between the regions $r \to 0$ and $r \to \infty$ is

$$Z_{\text{eff}}^{\ell} = 1 + (Z-1)e^{-a_1^{\ell}r} - r(a_3^{\ell} + a_4^{\ell}r)e^{-a_2^{\ell}r}, \qquad (2.21)$$

where the parameters $a_1^{\ell}, \ldots, a_4^{\ell}$ are found by fitting the experimental values of atoms energies to the ones predicted by a Hamiltonian with a model potential including this effects[6]. In most of the cases this values are fitted up to $\ell = 3$ as states with higher angular momentum do not have larger amount of penetration to the core electronic distribution, and thus the change in the effect compared to the state $\ell = 3$ is small.

As a matter of fact, it is common to call the states with angular quantum number greater than the angular quantum number of the core electrons $\ell > \ell_{\text{core}}$ non-penetrating states; hence experimentally one can use high-ℓ non-penetrating states to diminish the effect of penetration of the valence electron to the electronic core. This can be seen in the right panel of figure 2.2a where fast exponential decay of the effect for large quantum numbers is shown. For all the atoms in the figure, the behavior has the same qualitative characteristic. This is related to the overlap between the wavefunctions of the electronic core and the valence electron: as the valence electron gets in a higher ℓ-state, the wavefunction concentrates outside the core electrons leading to a suppression of the effect, as shown in figure 2.2b.

2.1.3 Effective Model Potential

In the past two subsections, we saw how the assumption of a distinguishable valence electron from the core electrons, as stated in equation (2.11), led to simplifications in the Coulomb interaction potential V_{ee} between all the electrons in the atom. This
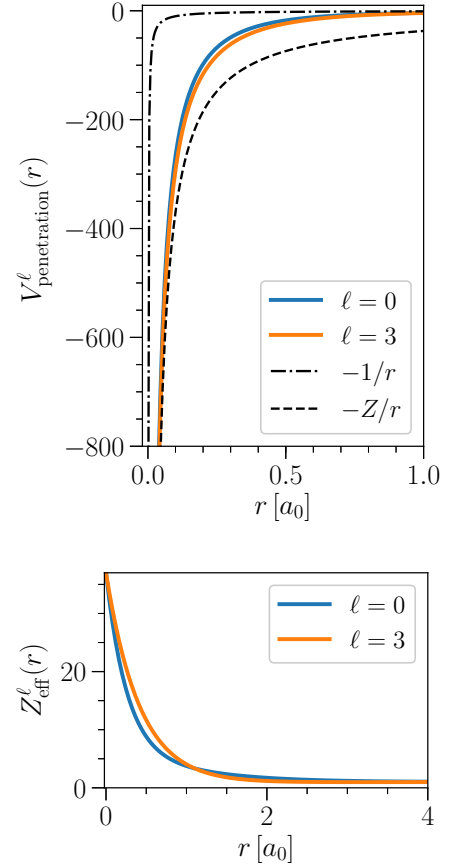

Figure 2.3: Penetration potential $V_{\text{penetration}}$ (top) and effective atomic number Z_{eff} (bottom) for Rubidium (Z=37). Here a_0 is the Bohr radius.

[6] See [13] for complete details.

assumption heavily relies on the fact that the core electrons are not dynamically involved in any of the transitions of interest and also that the valence electron is in a high-ℓ angular momentum state. Both of this assumptions are true for Alkali metal atoms or ionized Alkali earth metals where there is only one valence electron and the core electrons are in closed electronic subshells. This valence electron can then be excited to a high-ℓ Rydberg state and the properties of such state will then be well described by an effective model potential that effectively captures the multi-electron effects described before.

In this order of ideas, the portion $H_{\text{valence}} + V_{\text{int}}$ responsible for the valence electron dynamics and its interactions with the core electrons, equation (2.7) and equation (2.10) respectively, in the atomic Hamiltonian (2.6) can be casted into an effective central-field Hamiltonian

$$H_{\text{CF}} = \frac{p^2}{2\mu} + V_{\text{CF}}(r), \tag{2.22}$$

where the potential

$$V_{\text{CF}}(r) = V_{\text{pen}}(r) + V_{\text{pol}}(r) \tag{2.23}$$

includes the charge screening effects of the nucleus on the valence electron as well as the polarization effects due to the presence of the charge distribution of the core electrons.

As is, the central-field Hamiltonian (2.22) describes perturbatively the multi-electron effects on the valence electron as deviations from the hydrogenic model accounted for in the central-field potential V_{CF}. Although the origin of the penetration and polarization potential is well known and can be calculated exactly, the central-field Hamiltonian can also be used when a parametric model as core wavefunctions are usually not available. In this sense, the central-field Hamiltonian becomes a fit model to the experimental one-electron energy levels [13] that can describe highly excited electronic stated without the need of extensive calculations.

This approach also provides a computational advantage. We can rewrite the Hamiltonian (2.6) of the full atomic system as

$$H = H_{\text{core}} + H_{\text{CF}} + V_{\text{IS}}, \tag{2.24}$$

where the core eigenstates φ_γ^C and eigenenergies E_γ^C have to be calculated via a Hartree-Fock type calculation but, by knowing the parameters of the model potential, one can numerically calculate the eigenergies $E_{n\ell}^{\text{CF}}$ and eigenfunctions of the central-field Hamiltonian where all the multi-electronic effects are included perturbatively [14]. In this sense, the ionization energy of the state with quantum numbers $\gamma n\ell$ is

$$E_{\gamma,n\ell} = E_\gamma^C + E_{n\ell}^{\text{CF}} + \left\langle \Psi_{\gamma,n\ell} | V_{\text{IS}} | \Psi_{\gamma,n\ell} \right\rangle, \tag{2.25}$$

implying that the transition frequency between levels with the same core state γ but different state $n\ell$ for the valence electron are independent of the Hartree-Fock eigenenergies E_γ^C. In fact in many approaches the complete Hartree-Fock Hamiltonian H_{core} is discarded as is not important to discuss the properties of the transitions of the valence electron. However, H_{core} is responsible for the polarizability parameters of the model potential through its wavefunctions φ_γ^C as shown in equation (2.16). Since we are interested in the IS and the Hamiltonian is influenced by nuclear effects, here we cannot disregard it here.

2.2 Nuclear Effects

Atomic electrons are sensitive to the properties of the nucleus they are bound to, this sensitivity being reflected in the atomic transition energies. A very precise determination of atomic spectra can uncovers then information about the nucleus and its constituents. This is the case for example for exotic effects at the borderline between atomic and nuclear physics [15], such as parity violation in atomic transitions due to the weak interaction, are of interest. However, to be able to correctly disentangle this fancy phenomena, one should have a good understanding of the nuclear effects.

This section shortly introduces some of the nuclear effects on atomic transitions that are relevant for this work.

2.2.1 Normal Mass Shift

The effect of the nuclear motion relatively to the CM of the atom occurs already in one-electron atoms when the aproximation of infinite mass nucleus, as in Bohr's theory, is not assumed. For a nucleus with finite mass, the energy levels $E_n^{(\mu)}$ will be modified respect to the Bohr's atom energy levels $E_n^{(\infty)}$ by replacing the electron mass m_e by the reduced mass $\mu^{-1} = m_A^{-1} + m_e^{-1}$ of the atom[7]

[7] Compare with equation (2.1).

$$E_n^{(\mu)} = -\frac{\mu}{2\hbar^2}\left(\frac{e^2}{4\pi\epsilon_0}\right)^2 \frac{Z^2}{n^2} = -(2\pi\hbar)R^{(\mu)}\frac{Z^2}{n^2}. \qquad (2.26)$$

In general this effect can be recasted onto the Rydberg constant of each specific isotope

$$R^{(\mu)} \equiv \frac{\mu}{m_e}R^{(\infty)}, \qquad (2.27)$$

which translates into a renormalization of the Bohr's atom trasition frequencies by the ratio μ/m_e

$$\nu_{n\to n'}^{(\mu)} = R^{(\mu)}\left(\frac{Z^2}{n} - \frac{Z^2}{n'}\right) = \frac{\mu}{m_e}R^{(\infty)}\left(\frac{Z^2}{n^2} - \frac{Z^2}{n'^2}\right) = \frac{\mu}{m_e}\nu_{n\to n'}^{(\infty)}. \qquad (2.28)$$

This effect is called Normal Mass Shift (NMS) because it is the portion of the mass shift that corresponds to the variation of the reduced mass of the atom. Quantitatively, the latter means that the Bohr's atom energy levels $E_n^{(\infty)}$ are modified by the NMS as

$$\delta E_{\text{NMS}} = E_n^{(\infty)} - E_n^{(\mu)}$$

$$= -(m_{\text{e}} - \mu) \frac{1}{2\hbar^2} \left(\frac{e^2}{4\pi\epsilon_0} \right)^2 \frac{Z^2}{n^2}$$

$$= \left(1 - \frac{\mu}{m_{\text{e}}} \right) E_n^{(\infty)}; \qquad (2.29)$$

This also implies that the NMS decreases for heavier atoms with atomic number A as[8]

$$\frac{\delta E_{\text{NMS}}}{E_n^{(\infty)}} \approx \frac{m_{\text{e}}}{m_A} \approx \frac{m_{\text{e}}}{m_{\text{p}}} \frac{1}{A} \sim \frac{10^{-3}}{A}, \qquad (2.30)$$

and that the NMS affects homogeneously all of the atomic states.

We can see then that in our atomic Hamiltonian (A.4), the NMS effect appears in kinetic terms of the form $\frac{1}{2\mu} \sum_{i=1}^{N} p_i^2$.

2.2.2   Mass Polarization or Specific Mass Shift

When the system has more than two particles, the center of mass of any particular electron and the nucleus is no longer the center of mass of the whole system. When moving to the CM frame, there appears a set of two-body terms

$$\frac{1}{2m_A} \left\langle \Psi_{\gamma, n\ell} \middle| \mathbf{p}_i \cdot \mathbf{p}_j \middle| \Psi_{\gamma, n\ell} \right\rangle. \qquad (2.31)$$

in Hamiltonian (A.4), also called mass polarization terms, which imply a correction to the energy of the system

$$\Delta E_{\text{SMS}} = \frac{1}{2m_A} \sum_{i=1}^{N} \sum_{j \neq i}^{N} \left\langle \Psi_{\gamma, n\ell} \middle| \mathbf{p}_i \cdot \mathbf{p}_j \middle| \Psi_{\gamma, n\ell} \right\rangle. \qquad (2.32)$$

This effect is strongly dependent on the state of the atom, thus called the Specific Mass Shift (SMS). Since in momentum space the matrix elements of the momentum operators $\mathbf{p}_i$ can be expressed in terms of the matrix elements $\mathbf{r}_i$ between two states a and b as $\langle a | \mathbf{p}_i | b \rangle = -im\omega_{ab} \langle a | \mathbf{r} | b \rangle$, the operator $\mathbf{p}_i \cdot \mathbf{p}_j$ resembles the product of two dipole transition operators [16]. This is helpful to gain some insight on the SMS. Consider the separated wavefunction of valence and core electrons (2.11), let us split the sum above into the terms acting on the valence electron and the

[8] Here the nuclear mass m_A is approximated as $m_A = Zm_{\text{p}} + (A - Z)m_{\text{n}} \approx Am_{\text{p}}$.

core electrons, such that

$$\Delta E_{\text{SMS}} = \frac{1}{2m_A} \sum_{i=1}^{N_c} \sum_{j \neq i}^{N_c} \langle \varphi_\gamma^C | \mathbf{p}_i \cdot \mathbf{p}_j | \varphi_\gamma^C \rangle$$
$$+ \frac{1}{m_A} \sum_{i=1}^{N_c} \langle \varphi_\gamma^C | \mathbf{p}_i | \varphi_\gamma^C \rangle \cdot \langle \psi_{n\ell} | \mathbf{p} | \psi_{n\ell} \rangle. \qquad (2.33)$$

It is easy to see that the second term in the right-hand side vanishes, as $\langle \psi_{n\ell} | \mathbf{p} | \psi_{n\ell} \rangle$ is zero[9]. In a broader sense, this means that the SMS vanish between single particle product-type wave functions unless the matrix element is allowed by dipole selection rules. However, this is not the case for the wavefunctions φ_γ^C as they are not separable in the case of self-consistent Hartree-Fock type calculations, implying that the SMS for many-electron atom is due to the presence of electron correlations in the wavefunction as well as electron-electron exchange effects [17].

On the other hand, the SMS effect is also weigthed by $1/m_A$ as in the case of the NMS, hence for heavier atoms the size of the SMS effect decreases.

2.2.3 Field (or Volume) Shift

Since different isotopes of the same element have different number of neutrons, their nuclear charge distribution $\sigma(r)$ will not coincide, leading to a small shift in their electronic level energies; this is the so-called Volume Shift or Field Shift (FS). Inside the nucleus, the electrostatic potential no longer behaves like Ze/r but will be determined by the distribution of the nuclear charge.

To see that, consider the term $\sum_{i=1}^N V_{eN}(\mathbf{r}_i)$ in the many-electron atom Hamiltonian (A.4). This term can encapsulate a correction to the point-like Coulomb interaction between the electrons and the nucleus; The first-order shift of the energy levels due to the replacement of the pointlike nuclear distribution $\sigma = Z\delta^{(3)}(\mathbf{r}_N)$ by an extended nucleus charge distribution $\sigma(\mathbf{r})$

$$\delta E_{\text{FS}} = \int d^3r \int d^3r' \frac{Z\delta^{(3)}(\mathbf{r}')}{|\mathbf{r} - \mathbf{r}_N|} \rho(\mathbf{r}) - \int d^3r \int d^3r' \frac{\sigma(\mathbf{r}')}{|\mathbf{r} - \mathbf{r}'|} \rho(\mathbf{r}), \qquad (2.34)$$

where $\rho(\mathbf{r})$ is the electron density, and

$$\int d^3r\, \sigma(\mathbf{r}) = Z. \qquad (2.35)$$

If one assumes that the nucleus has no permanent electric dipole $\int d^3r_N\, \mathbf{r}_N \rho_N(\mathbf{r}) = 0$, the expression above reduces to[10]

$$\delta E_{\text{FS}} = \frac{2\pi}{3} Ze^2 \rho(0) \langle r_N^2 \rangle \qquad (2.36)$$

where $\langle r_N^2 \rangle$ is the root mean square radius of the nuclei and $\rho(0)$ is the electron density at the nucleus.

[9] Note that the assumption of the separability of the wavefunction in equation (2.11) neglects any correlation effects between the core electrons and the valence electron. In a more general scenario, electron correlations due to configuration mixing can also lead to SMS effects even if the states do not fulfill the dipole selection rules.
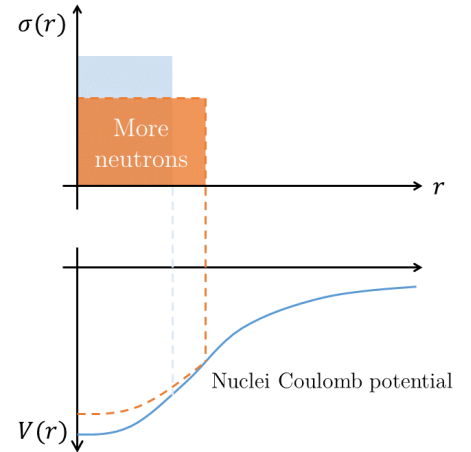

Figure 2.4: Simplified picture of the Field Shift due to the change of the nuclear volume.

[10] See §90.1.1 in Reference [17] for a detailed calculation.

Several models for the nuclear charge distribution have been used in the literature to describe the behavior of the nuclear density. Experiments have demonstrated that is actually the root mean square radius $\langle r_N^2 \rangle^{1/2}$ of the nuclear charge distribution, rather than the charge distribution itself, the parameter responsible for the Field Shift—as given in equation (2.36). Other moments of the nuclear charge distribution also contribute but are of smaller scale [18], regardless they become important when the hyperfine structure[11] of the atom is relevant.

[11] Hyperfine structure arises from the interaction between the nuclear magnetic dipole moment and the magnetic field generated by the electrons as well as the energy of the nuclear electric quadrupole moment in the electric field gradient due to the distribution of charge within the atom.

The scaling of the FS is polynomial in m_A, contrary to the inverse-power dependence on the SMS and NMS, and depends strongly on the quantum state of the atom through the electron density in the nucleus $\rho(0) = |\Psi_{\gamma,n\ell}(0)|^2$. Especially the *s*-electronic orbitals, which have the largest overlap with the nucleus, will experience more FS.

Consider now the term V_{nucleus} in equation (2.9) of the many-electron Hamiltonian. This potential describes the interaction of the valence electron with the nucleus and will then be responsible to account for the Field Shift effect. Now, if the valence electron is in a high-ℓ state, then its electron density in the nucleus is zero, and the valence electron will not experience any Field Shift. This is true however to first approximation. Looking at the core Hamiltonian (2.8) one can see an interaction term V_{eN} between the core electrons and the nuclei. As this Hamiltonian is responsible for the core wavefunctions φ_γ^C and in turn this wavefunctions determine the parameters of the model potential (2.16), then there exists a next-to-leading field shift in the valence electron that is hidden within it.

This higher-order effect of the FS on the parameters is expected to be small. However it is important to be able to quantify the effect as it does not scale proportionally to the mass like the NMS and SMS, and then cannot be factorized as such.
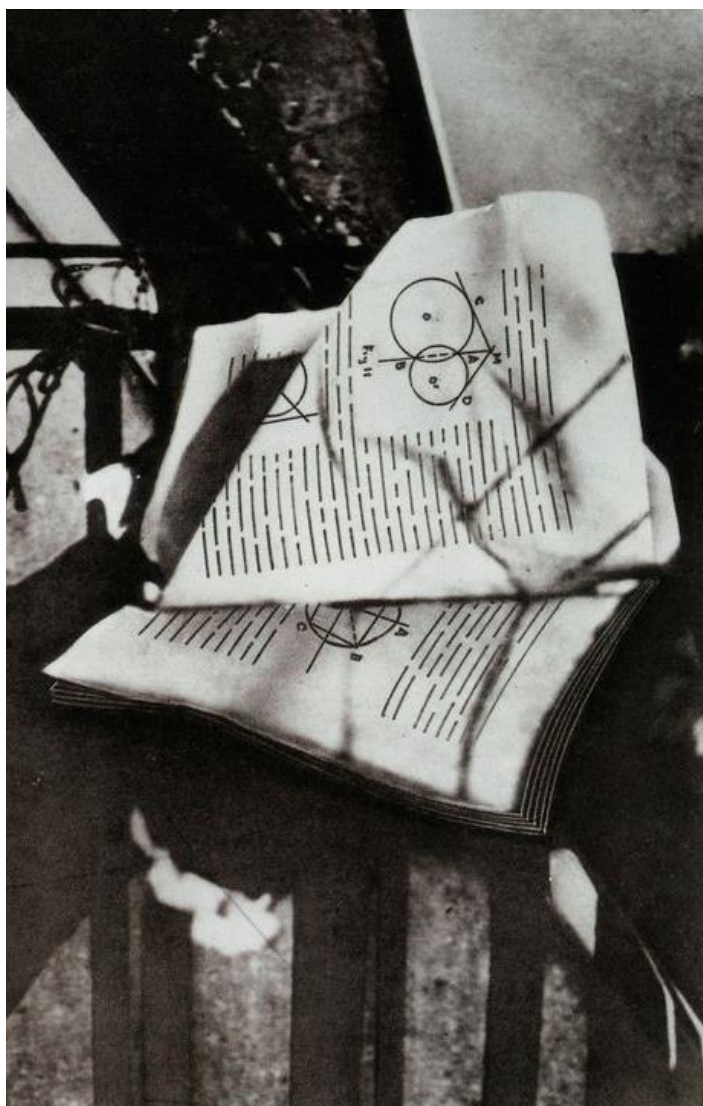
Marcel Duchamp's Unhappy Readymade. 1919.

Chapter 3

Extracting Data from Experiments

Using experimental data, one can extract information about the nuclear and electronic properties of the atom. In the nuclear case one can use the data from different isotopes of the same element to extract the Mass Shift and Field Shift contributions. In a similar manner, by measuring the energy difference between different angular momentum states of an atom, it is possible to extract information about the polarizabilities.

3.1 Separation of Electronic Effects: The Polarization Plot

As described in §2.1, high-ℓ states of the valence electron with negligible overlap with the core are dominated by polarization effects described by the potential (2.17),

$$V_{\mathrm{pol}}(r) = -\frac{\alpha^{E1}}{2r^4} - \frac{\alpha^{E2}}{2r^6}. \tag{3.1}$$

The energy difference between two levels with angular quantum numbers ℓ and ℓ' but same principal quantum number n is given by

$$\Delta E_{n\ell \to n\ell'} = \frac{\alpha^{E1}}{2}\Delta\left\langle r^{-4}\right\rangle_{\wp} + \frac{\alpha^{E2}}{2}\Delta\left\langle r^{-6}\right\rangle_{\wp}, \tag{3.2}$$

where $\wp \equiv n\ell \to n\ell'$ is the transition and $\Delta\left\langle r^{-\kappa}\right\rangle_{\wp} = \left\langle r^{-\kappa}\right\rangle_{n\ell'} - \left\langle r^{-\kappa}\right\rangle_{n\ell}$.

One can then find a linear relation

$$\frac{\Delta E_{\wp}}{\Delta\left\langle r^{-4}\right\rangle_{\wp}} = \frac{\alpha^{E1}}{2} + \frac{\alpha^{E2}}{2r^4}\frac{\Delta\left\langle r^{-6}\right\rangle_{\wp}}{\Delta\left\langle r^{-4}\right\rangle_{\wp}} \tag{3.3}$$

where the set of points for different ℓ and ℓ' states with fixed n will give the dipole polarizability coefficient as the intercept of the line and the quadrupole polarizability coefficient as the slope. This is the so-called a polarization plot [7].

However, higher order effects of the polarizability expansion can lead to errors and, under real experimental conditions, other effects might be important and will modify the shape of the model
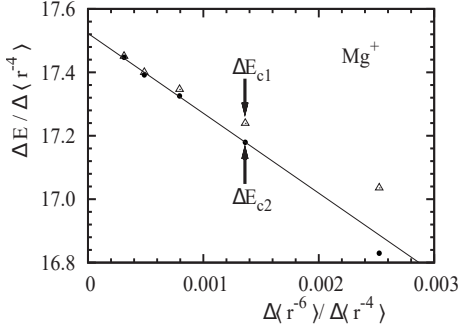
(a) Mg^+ for the $n = 17$ Rydberg levels. The linear regression for the ΔE_{c2} plot did not include the last point.
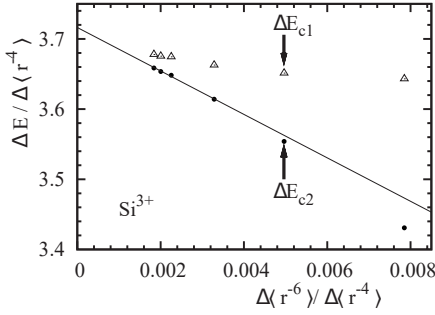
(b) Si^{3+} for the n=29 Rydberg levels. The linear regression for the ΔE_{c2} plot did not include the last two points.

Figure 3.1: The polarization plot of the fine-structure intervals of Mg^+ (a) and Si^{3+} (b). The ΔE_{c1} intervals are corrected for relativistic, second-order, and Stark shifts. The ΔE_{c2} intervals account for $\langle r^{-7} \rangle$ and $\langle r^{-8} \rangle$ polarizability effects. Plots taken from reference [19].

potential [7, 19]. Such new terms in the model potential include relativistic effects E_{rel}, Stark shifts from ambient electric fields E_{ss}, second-order effects due to relaxation of the Rydberg electron in the field of the polarization potential E_{sec} and, as mentioned, corrections due higher order polarizabilities of the ionic core. To circumvent the problem one can calculate and subtract these higher order effects from the observed experimental values

$$\frac{\Delta E_\wp^{calc}}{\Delta \langle r^{-4} \rangle_\wp} = \frac{\Delta E_\wp^{obs}}{\Delta \langle r^{-4} \rangle_\wp} - \frac{\Delta E_{HO}}{\Delta \langle r^{-4} \rangle_\wp}, \tag{3.4}$$

where ΔE_{HO} is the calculated energy shift due to higher order effects. This leads to a new linear relation

$$\frac{\Delta E_\wp^{calc}}{\Delta \langle r^{-4} \rangle_\wp} = \frac{\alpha^{E1}}{2} + \frac{\alpha^{E2}}{2} \frac{\Delta \langle r^{-6} \rangle_\wp}{\Delta \langle r^{-4} \rangle_\wp}. \tag{3.5}$$

The effects of this higher order corrections in the linearity is shown in figure 3.1.

Another option to go around the higher order polarizability effects and minimize them is to use high-ℓ states, as $\langle r^{-\kappa} \rangle \sim l^{-2\kappa}$ renders the effect negligible. However, as the higher order corrections get lower with higher ℓ and n, the states become more sensitive to stark shifts from stray electric fields, with the sensitivity (polarizability) scaling as n^7. One has to choose then ℓ states that suppresses the higher order effects but are not too sensitive to stray electric fields [7]. Nevertheless there are new techniques that can reduce the sensitivity to stray electric fields of the chosen states [20] that could allow a measurement of this linear behavior in high-ℓ states where higher order effects are suppressed.

3.2 Separation of Nuclear Effects: Isotope Shift and the King's Plot

In §2.2 we described the energy shifts on the atomic spectra due to nuclear effects. This effects appear because of the difference between the masses and the volume of the nuclei for different isotopes, and thus called Isotope Shifts (IS).

Take for example the Normal Mass Shift (NMS) on §2.2.1. Consider two isotopes of the same species, with A and A' being their atomic mass numbers. These two isotopes of reduced masses μ and μ' will have for the same transition $\wp \equiv n\ell \rightarrow n'\ell'$ a different NMS. The difference between this two transitions corresponds to the isotope shift induced by the NMS on each single atom.

Quantitatively, the fractional difference of the transition frequency (or IS) due to the NMS between two Isotopes of reduced

masses μ and μ' is

$$\frac{(\Delta\nu_\wp)^{AA'}_{\text{NMS}}}{\nu_\wp^{(\mu)}} \equiv \frac{\nu_\wp^{(\mu')} - \nu_\wp^{(\mu)}}{\nu_\wp^{(\mu)}} = \frac{\mu'}{\mu} - 1 = \frac{m_e}{m_A}\frac{m_A - m_{A'}}{m_e + m_{A'}}, \qquad (3.6)$$

with $\nu_\wp^{(\mu)}$ given by equation (2.28). The fractional shift by the NMS is[12]

$$\frac{(\Delta\nu_\wp)^{AA'}_{\text{NMS}}}{\nu_\wp^{(\mu)}} \approx \frac{m_e}{m_p}\frac{A - A'}{AA'} \approx 5.45 \times 10^{-4}\frac{A - A'}{AA'}. \qquad (3.7)$$

Then isotope shift due to the NMS rapidly decreases for heavy atoms as A^{-2} when the difference between the isotopes mass number A and A' is not too big, and it is weighted by the electron-proton mass ratio. This value is known with a relative uncertainty of $\mathcal{O}(10^{-11})$ [21] and then the NMS can be precisely predicted [13] and, because of it, usually scaled out.

On the other hand, the Specific Mass Shift (SMS) described in §2.2.2 for the same transition $\wp$ will lead to an Isotope Shift [17, §16.2.1]

$$(\Delta\nu_\wp)^{AA'}_{\text{SMS}} = K_\wp \mu^{-1}_{AA'} \quad \text{with} \quad \mu^{-1}_{AA'} = \frac{m_A - m_{A'}}{m_A m_{A'}} \qquad (3.8)$$

where $K_\wp = \langle\Psi_{\gamma,n\ell}|\sum_{i<j}\mathbf{p}_i \cdot \mathbf{p}_j|\Psi_{\gamma,n\ell}\rangle - \langle\Psi_{\gamma',n'\ell'}|\sum_{i<j}\mathbf{p}_i \cdot \mathbf{p}_j|\Psi_{\gamma',n'\ell'}\rangle$ is a purely electronic factor. In addition, notice that this expression scales as the NMS due to the mass factor, then the NMS and SMS are expected to have the same order of magnitude. However, accurate determination of the SMS is difficult due to its dependency on the core electron wavefunctions in contrast to the NMS.

The two IS mechanism discussed above rapidly decrease with increasing A. It is then suggestive to use heavy atoms to minimize the effects of IS but, as the atoms becomes heavier, the Field Shift (FS) effect becomes important. As described in §2.2.3, the FS can be separated as well into an electronic factor, proportional to the electronic density at the origin $\rho(0)$, times a nuclear factor, the root mean square radius of the nuclear charge distribution. Thus, the isotope shift due to the FS for a transition $\wp$ can be written as

$$(\Delta\nu_\wp)^{\mu\mu'}_{\text{FS}} = F_\wp \lambda^{AA'}, \qquad (3.9)$$

where the term $F^\wp$ is the electronic factor proportional to $\Delta\rho(0) = |\Psi_{\gamma,n\ell}|^2 - |\Psi_{\gamma',n'\ell'}|^2$ between the initial and final electronic states, which in the simplest perturbation approach is given by $(2\pi/3)Ze^2\Delta\rho(0)$ as shown in (2.36).

The nuclear factor $\lambda^{AA'}$ is proportional to the root mean square radius of the nuclear charge distribution, but more generally it should include all the moments of the nuclear distribution, such

[12] Where nuclear mass m_A was approximated as $m_A = Zm_p + (A - Z)m_n \approx Am_p$.

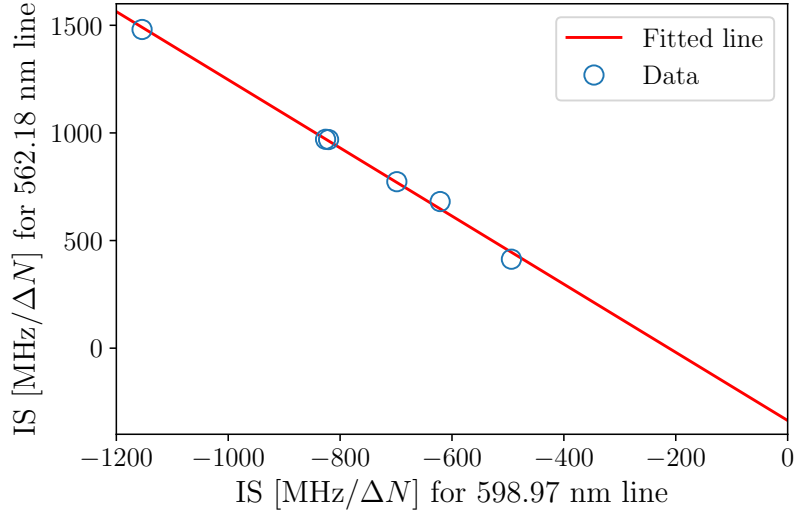[13] See Ref. [22], page 226 of Ref. [16] and §16.2.1 of Ref. [17]

FIGURE 3.2: King's plot for Samarium transitions. The transitions are normalized by the difference of neutron number. The linear regression gives slope $m = -1.582$ and intercept $c = -335.95$.

that

$$\lambda^{AA'} = \delta \left\langle r_N^2 \right\rangle^{AA'} + (C_2/C_1)\delta \left\langle r_N^4 \right\rangle^{AA'} + (C_3/C_1)\delta \left\langle r_N^6 \right\rangle^{AA'} + \cdots,$$
(3.10)

with $\delta \left\langle r_N^k \right\rangle^{AA'} = \left\langle r_N^k \right\rangle^A - \left\langle r_N^k \right\rangle^{A'}$ being the difference of the average value of nuclear charge distribution r^k between two isotopes with atomic numbers A and A'. The ratios C_i/C_1 ($i = 1, 2, \dots$), which weight the higher even moments, depend only on Z and not on the particular transition [17, §16.2.3].

With all of the above, the total IS of an spectral line $\wp$ will be given by the sum of the mass dependent effects, the NMS and SMS, and the volume effect FS, and can be written as

$$(\Delta \nu_\wp)^{AA'} = (\Delta \nu_\wp)_{\text{NMS}}^{\mu\mu'} + K_\wp \mu_{AA'}^{-1} + F_\wp \lambda^{AA'}.$$
(3.11)

In general, as the NMS can be determined with very high precision and acts homogeneously on all the transitions, it can then be factorized out, yielding the *scaled* or *reduced* IS

$$(\Delta \nu_\wp)^{AA'} = K_\wp \mu_{AA'}^{-1} + F_\wp \lambda^{AA'}.$$
(3.12)

Analytical knowledge of the factor in the expression above are not known, and one should extract information about them from available experimental data.

3.2.1 King's Plot

A method used to separate the mass shift and field shift from experimentally measured data is based on the King's plot [23, 24]. By using two different transitions the King's plot exploits the relations between the electronic and atomic factors in (3.12) to extract ratios and differences between them, and without knowledge of the cumbersome nuclear factors $\lambda^{AA'}$.

Consider two spectral lines $\wp$ and $\wp'$ for a defined pair of isotopes A and A'. If one assumes that the proposed separability in equation (3.12) is valid[14] then, by taking the two spectral lines

$$(\Delta\nu_\wp)^{AA'} = K_\wp \mu_{AA'}^{-1} + F_\wp \lambda^{AA'} \quad \text{and}$$
$$(\Delta\nu_{\wp'})^{AA'} = K_{\wp'} \mu_{AA'}^{-1} + F_{\wp'} \lambda^{AA'} \tag{3.13}$$

one can find a relationship between the shifts of the spectral line $\wp$ and $\wp'$. Since $\lambda^{AA'}$ is independent of the transitions[15], we can write it in terms of $(\Delta\nu_\wp)^{AA'}$, $K_\wp$, and $F_\wp$ as

$$\lambda^{AA'} = \frac{1}{F_\wp}(\Delta\nu_\wp)^{AA'} - \frac{K_\wp}{F_\wp}\mu_{AA'}^{-1} \tag{3.14}$$

and then replaced into the isotope shift for spectral line $\wp'$, leading to

$$(\Delta\nu_{\wp'})^{AA'} = \left(\frac{F_{\wp'}}{F_\wp}\right)(\Delta\nu_\wp)^{AA'} + \left[\left(K_{\wp'} - \frac{K_\wp}{F_\wp}\right)\mu_{AA'}^{-1}\right]. \tag{3.15}$$

The equation above defines a linear relation between $(\Delta\nu_\wp)^{AA'}$ and $(\Delta\nu_{\wp'})^{AA'}$ where the slope of the line is the ratio of the electronic F-factors and the intercept is the relation between the mass polarization K-factors. Each pair of A and A' isotopes defines a point; a set of such points forms the King's plot. To trace linearity, we must consider at least 4 isotopes $(A; A_1; A_2; A_3)$ forming 3 pairs, giving three points on the plot. For example [25, §1.9], the linear regression of various pairs of Sm (samarium) isotopes for the spectral lines 562.18 nm $^7F_1 \to^7 H_2$ and 598.97 nm $^7F_0 \to^7 D_1$ have the linear behavior shown in figure 3.2. Such a plot, a diagram where the scaled IS of a line $\wp$ is plotted against the IS of another line $\wp'$, is called a King's plot.

Atomic approaches to search for new physics rely on the assumption that the linearities above hold. In the case that a new force carrier appears a linearity breaking is expected in the polarization plot, due to the influence of the new mediator with the electronic properties, as well in the King's plot, in this case through the modification of the isotopes shift formula due to the possible nuclear coupling of the new mediator with the nucleus. In the following section the aforementioned new physics mediator will be introduced and then its influence on the atomic spectra and the linear relations above discussed.

[14] Non-linear corrections to the King's plot may be due to the non-factorization of the electronic and nuclear parameters in the expression for the FS [3].

[15] See discussion around equation (3.9).

"¿De qué trata el experimento?, dijo Rosa. ¿Qué experimento?, dijo Amalfitano. El del libro colgado, dijo Rosa. No es ningún experimento, en el sentido literal de la palabra, dijo Amalfitano. ¿Por qué está allí?, dijo Rosa. Se me ocurrió de repente, dijo Amalfitano, la idea es de Duchamp, dejar un libro de geometría colgado a la intemperie para ver si aprende cuatro cosas de la vida real. Lo vas a destrozar, dijo Rosa. Yo no, dijo Amalfitano, la naturaleza. Oye, tú cada día estás más loco, dijo Rosa. Amalfitano sonrió. Nunca te había visto hacerle una cosa así a un libro, dijo Rosa. No es mío, dijo Amalfitano. Da lo mismo, dijo Rosa, ahora es tuyo. Es curioso, dijo Amalfitano, así debería ser pero lo cierto es que no lo siento como un libro que me pertenezca, además tengo la impresión, casi la certeza, de que no le estoy haciendo ningún daño. Pues haz de cuenta que es mío y descuélgalo, dijo Rosa, los vecinos van a creer que estás loco. ¿Los vecinos, los que ponen trozos de vidrio encima de las tapias? Ésos ni siquiera saben que existimos, dijo Amalfitano, y están infinitamente más locos que yo. No, ésos no, dijo Rosa, los otros, los que pueden ver perfectamente bien lo que pasa en nuestro patio. ¿Alguno te ha molestado?, dijo Amalfitano. No, dijo Rosa. Entonces no hay problema, dijo Amalfitano, no te preocupes por tonterías, en esta ciudad están pasando cosas mucho más terribles que colgar un libro de un cordel. Una cosa no quita la otra, dijo Rosa, no somos bárbaros. Deja el libro en paz, haz de cuenta que no existe, olvídate de él, dijo Amalfitano, a ti nunca te ha interesado la geometría."

—2666, Roberto Bolaño.

"What's the experiment about?, asked Rosa. What experiment? asked Amalfitano. With the hanging book, said Rosa. It isn't an experiment, in the literal sense of the word, said Amalfitano. Why is it there?, asked Rosa. It came to me all of a sudden, said Amalfitano, it's a Duchamp's idea, leaving a geometry book hanging exposed to the elements to see if it learns some facts about real life. You're going to destroy it, said Rosa. Not me, said Amalfitano, nature. You're getting crazier every day, you know, said Rosa. Amalfitano smiled. I've never seen you doing a thing like that to a book, said Rosa. It isn't mine, said Amalfitano. It doesn't matter, Rosa said, it's yours now. It's funny, said Amalfitano, that's how I should feel, but I really don't have the sense it belongs to me, and anyway I have the impression, almost the certainty, that I'm not doing it any harm. Well, pretend it's mine and take it down, said Rosa, the neighbors are going to think you're crazy. The neighbors, those who top their walls with broken glass? They don't even know we exist, said Amalfitano, and they're way crazier than me. No, not them, said Rosa, the other ones, those ones who can see exactly what's going on in our yard. Have any of them bothered you? asked Amalfitano. No, said Rosa. Then it's not a problem, said Amalfitano, it's silly to worry about such small things when worse things are happening in this city other than a book being hung from a cord. One does not exclude the other, said Rosa, we're not barbarians. Leave the book alone, pretend it doesn't exist, forget about it, said Amalfitano, you've never been interested in geometry." _{*(free translation)}

—*2666*, Roberto Bolaño.

Chapter 4

New Long-Range Interactions

The Standard Model of particle physics (SM) successfully describes and predict numerous phenomena up to the TeV scale, and it is theoretically consistent up to a much higher energy. However, the SM has major problems as it cannot account for other experimentally observed phenomena. For example, it has no dark matter particle that can explain observational measurements of gravitational interaction, it cannot explain the baryonic assymetry or imbalance of matter anti-matter in the observable universe, nor it can predict neutrino oscillations. The above provides a strong motivation to look for new particles beyond those included in the SM. Although in the search of New Physics (NP) efforts concentrate in colliders and high-intensity experiments, optical tabletop experiments can also be used as new high-precision approaches to probe low-energy NP processes [1].

A systematic way to search for the effects of NP on atomic systems and quantify their existence or lack thereof relies on the measurement of the coupling constants of this new exotic physics. Then, in a broad sense, the goal of an experiment is to search for an exotic interaction and, if nothing is found, a limit or constraint is established for the coupling constants of the particular form of such interaction. Atomic experiments seek to explore regions of parameter space that have not been previously studied to determine if undiscovered physics exists with such properties. In the aftermath particle theorists can interpret the experimental results in terms of possible new particles and derive limits on beyond the SM theories.

Throughout this section the natural units system is used $\hbar = c = 1$ unless otherwise stated.

4.1 Long-Range Fermion Interactions

Consider the long range force between two fermions mediated by a very light particle ϕ. The general form of the scattering amplitude is written in terms of the Lorentz invariant matrix element

$$\text{Im}\{\mathcal{M}\} = -\frac{1}{q_\alpha q^\alpha + m_\phi^2} \mathcal{S}(\vec{q}, \vec{p}), \qquad (4.1)$$

where q_μ is the four-momentum and m_ϕ the mass of the mediator particle ϕ.

The mathematical object above encodes all the properties of the force. The range of the interaction will be determined by the mass of the particle related to the Compton wavelength $\lambda_\phi = \hbar/m_\phi c$, this length-scale directly determines the sensitivity of an experiment probing the interaction to be on the $r_{\exp} \lesssim \lambda_\phi$. On the other hand, the coupling strength of the mediator ϕ to the fermions ψ and ψ' is given by the spin-dependent factor $\mathcal{S}(\vec{q}, \vec{p})$, where the spin properties of the interacting fermions will determine the type of the interaction and thus the character of the mediator [26].

In the low energy regime, the Fourier transform of the momentum-space amplitude (4.1) with respect to the momentum transfer $\vec{q}$ gives the position-space potential induced by the exchange of the particle ϕ is given by [27, §5.2]

$$V_\phi(\mathbf{r}) = - \int \frac{\mathrm{d}^3 q}{(2\pi)^3} e^{\mathbf{q}\cdot\mathbf{r}} \operatorname{Im}\{\mathcal{M}\}. \tag{4.2}$$

Notice that $V(\mathbf{r})$ is intrinsically not Lorentz invariant because it only involves integration over the spatial coordinates, however it reproduces the low-energy limit of the interaction that is of interest in atomic experiments.

To lowest order in the mass ratio between the interacting fermions and the boson exchanged $m_{\psi,\psi'}/m_\phi$, the New Physics potential will have the form [26]

$$V_\phi(r) = -k_{\mathrm{NP}} \frac{e^{-r/\lambda_\phi}}{r}, \tag{4.3}$$

such that the low-energy spin-independent limit of the force is determined by the non-relativistic Yukawa potential. The constant k_{NP} is related directly to the coupling between the fermions and the NP boson ϕ.
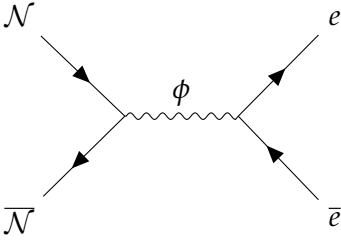

Figure 4.1: Scattering of electrons with nucleons $\mathcal{N}$ mediated by a low mass force carrier ϕ.

4.2 Breaking Linearity

Consider the case in which the NP mediator couples electrons to nucleons, that is, to protons and neutrons. The NP coupling constant will then be given by

$$k_{\mathrm{NP}} = (-1)^s \frac{y_e y_A}{4\pi}, \quad \text{where} \quad y_A = (A - Z)y_n + Z y_p \tag{4.4}$$

is the effective coupling of the nucleons and the NP mediator ϕ with spin $s = 0, 1, 2$ [15].

On one hand, the coupling y_p of the NP particle with protons implies a correction of the atomic Coulomb potential, the effects of such a coupling will be then screened by the multiple electron-electron interaction in the atom and then hidden in the electronic coefficients of a certain level. Thus, only experimental

observables sensitive to the electronic coefficients will be affected by such a coupling.

On the other hand, if the hypothetical new force couples electrons and neutrons, experiments sensitive to the variation of the coupling constant k_{NP} through the change in atomic number A will be sensitive to the NP potential.

The experimental observables describe in §3 can be used to extract information about the parameters of the new force carrier.

4.2.1 Polarization Plot

In section §3.1 the linear relation

$$\frac{\Delta E_\wp^{\text{calc}}}{\Delta \langle r^{-4}\rangle_\wp} = \frac{\alpha^{E1}}{2} + \frac{\alpha^{E2}}{2}\frac{\Delta \langle r^{-6}\rangle_\wp}{\Delta \langle r^{-4}\rangle_\wp}. \tag{4.5}$$

for high-ℓ states of the valence electron was derived. Now, considering the presence of the new hypothetical force mediator ϕ through an atomic potential (4.3), the linear relation above will be modified as

$$\frac{\Delta E_\wp^{\text{calc}}}{\Delta \langle r^{-4}\rangle_\wp} = \frac{\alpha^{E1}}{2} + \frac{\alpha^{E2}}{2}\frac{\Delta \langle r^{-6}\rangle_\wp}{\Delta \langle r^{-4}\rangle_\wp} + k_{NP}\frac{\Delta \langle r^{-1}e^{-r/\lambda_\phi}\rangle_\wp}{\Delta \langle r^{-4}\rangle_\wp}. \tag{4.6}$$

Contributions from the NP potential become comparable to the other terms of the expression above when terms of the order $r_{\text{exp}}^4/\lambda_\phi^4 \ll 1$ are relevant. For high-ℓ Rydberg orbitals, which are the focus of this work, the experimental sensitivity will be proportional to the orbit radius $r_{\text{exp}} \sim a_0\ell^2$, implying a sensitivity only to NP mediator with relatively low masses $m_\phi^{-1} \gg a_0^4\ell^8$. In that case, the overall effect of the NP potential will be of an effective correction to the Coulomb potential and, as such, not quantifiable with the Polarization Plot.

One can still rely on the precision to which the coefficients C_4 and C_6 are known to alleviate the requirements on m_ϕ^{-1}. However, error assessments in experiments extracting such coefficients is complicated and reach only precision on the order of tens of percent [19]. Even more, experimental data on the atoms of interest is limited and does not allow to build projection formulas for the coefficients of interest.

All in all, by using the polarization approach one purely relies on the electronic properties of the NP. This in turn sets the range to which the method will be sensitive to NP where only low mediator masses can be probed. On the other hand, to set bounds for any NP mediator one would require precise estimations of the model potential parameters which are not available for alkali atoms.

The future however is not completely obscure for this approach. Microwave spectroscopy data of high-ℓ states for the alkaline earth Mg^+ [28] and the noble gasses Ne [29] and Ar [30] is

available, opening the possibility towards the exploration of this elements as possible playgrounds.

4.2.2   Isotope Shift and King's Plot

Consider now the expression for the isotope shift (IS) in equation (3.12). With enough experimental accuracy, IS measurements become sensitive to the presence of the NP potential. In the presence of this new effect the, IS becomes [2]

$$(\Delta\nu_\wp)^{AA'} = K_\wp \frac{m_A - m_{A'}}{m_A m_{A'}} + F_\wp \lambda^{AA'} + \alpha_{\text{NP}} X_\wp \gamma_{AA'}, \qquad (4.7)$$

where $X_\wp$ is the electronic factor associated with the NP potential, $\gamma_{AA'}$ depends on the nuclear properties, and α_{NP} is proportional to the coupling of neutrons and electrons. Specifically, from equation (4.3) this coefficients are

$$\alpha_{\text{NP}} = (-1)^s \frac{y_e y_n}{4\pi}, \quad X_\wp = \left\langle \frac{e^{-r/\lambda_\phi}}{r} \right\rangle_\wp, \quad \text{and} \quad \gamma^{AA'} = AA'. \tag{4.8}$$

If one tries to construct a King's plot as in §3.2.1 from the IS formula above, one gets the following relation between the IS frequencies

$$(\Delta\nu_{\wp'})^{AA'} = \left(\frac{F_{\wp'}}{F_\wp}\right)(\Delta\nu_\wp)^{AA'} + \left[\left(K_{\wp'} - \frac{K_\wp}{F_\wp}\right)\mu_{AA'}^{-1}\right]$$
$$+ \alpha_{\text{NP}} X_\wp \left(\frac{X_{\wp'}}{X_\wp} - \frac{F_{\wp'}}{F_\wp}\right)\gamma^{AA'}, \tag{4.9}$$

where, as a consequence of the presence of the NP potential, there exist a deviation of linearity in the King's plot.

It is important to analyze the cases in which this explicit breaking of King's linearity is valid. On one hand, one must require that

$$\frac{X_{\wp'}}{X_\wp} \neq \frac{F_{\wp'}}{F_\wp}, \tag{4.10}$$

that is, that the NP force is not short-range, such that nuclear effects does not suppress the sensitivity to the new force mediator. On the other hand, some other non-linearities may appear from higher-order contributions of the nuclear and electronic-structure physics and, as we outlined before, these are usually hard to calculate, for as they are not completely understood. For example, one possible source of nonlinearities is of the form of a field shift that depends on the isotope mass [15].

If an experimental deviation from King's linear behavior is observed, due to the precision to which this higher-order effects are known, it will be difficult to distinguish the NP contributions and other sources of nonlinearity. However, further insight of

the NP can be gained if contributions from nuclear effects can be ruled out. In that case the fact that NP forces are of a longer range than nuclear effects can be beneficial. On the other hand, if linearity is observed, then with high certainty any NP contribution can be ruled out.

IS measurements of Rydberg states, highly excited electronic states, can provide electronic observables that circumvent the nuclear effects. The use of Rydberg states to provide IS observables independent of nuclear effects and that could possibly bound long-range NP mediators, which is the main objective of this thesis. This approach to bound NP and the construction of such observables is the subject of the following section.

"Morelliana.
Basta mirar un momento con los ojos de todos los días el comportamiento de un gato o de una mosca para sentir que esa nueva visión a que tiende la ciencia, esa des-antropomor-fización que proponen urgentemente los biólogos y los físicos como única posibilidad de enlace con hechos tales como el instinto o la vida vegetal, no es otra cosa que la remota, aislada, insistente voz con que ciertas líneas del budismo, del vedanta, del sufismo, de la mística occidental, nos instan a renunciar de una vez por todas a la mortalidad."

—*Rayuela*, Julio Cortázar.

"Morelliana.
It is enough to take a momentary look with everyday eyes at the behavior of a cat or a fly to feel that the new vision towards which science seems to be heading, that dis-anthropomor-phization urgently proposed by biologists and physicists as the only possible conjoinment with phenomena such as instinct or vegetal life, is nothing but the remote, isolated, insistent voice by which certain lines of Buddhism, Vedanta, Sufism, Western mysticism urge us to renounce mortality once and for all." *(free translation)

—*Hopscotch*, Julio Cortázar.

Chapter 5

Using Rydberg Atoms to Probe New Physics

Rydberg states, atomic states with high principal n and angular ℓ quantum number, are in general less affected by nuclear and electronic systematics than low lying atomic states, mainly due to the large orbital radius of the valance electron. In contrast, precise isotope shift (IS) measurements of optical transitions depend heavily on a detailed description of nuclear structure and are therefore very difficult to theoretically calculate. This suggest Rydberg states as a good platform for searches of new physics (NP) —light force mediators between neutrons in the nucleus and electrons— as they are potentially able to disentangle the new physics observable from nuclear effects. However isotope shifts of all multi-electron atoms are also affected by multi-electron correlations which, due to their many-body character, are also impossible to precisely evaluate and therefore affecting the precision of new physics measurements in Rydberg atoms.

5.1 Rydberg Atoms

Rydberg atoms [31], atoms in states of high principal quantum number n, are atoms with exaggerated properties, i.e., strong response to electric and magnetic fields, long decay periods and electron wavefunctions that approximate, under some conditions, classical orbits of electrons about the nuclei with extremely large radius.

Rydberg atoms have played an important role since the beginning of atomic physics. With their first appearance in the Balmer formula for the series of atomic Hydrogen, the empirical binding energies of the electron are given by the formula

$$W = -\frac{R}{(n - \delta_\ell)^2},$$

(5.1)

with R the Rydberg constant[16], n an integer, and δ_ℓ is an empirically observed quantum defect for the series of orbital angular momentum ℓ. This empirical formula was explained by the Bohr model (see §2), where n is the principal quantum number of the

[16] The Rydberg constant has recently shown to be of interest because its relation to the proton radius puzzle [32]. High precision measurement of the Rydberg constant independent from nuclear-charge-radius effects could help to bound the uncertainties in the measurement of the proton radius.
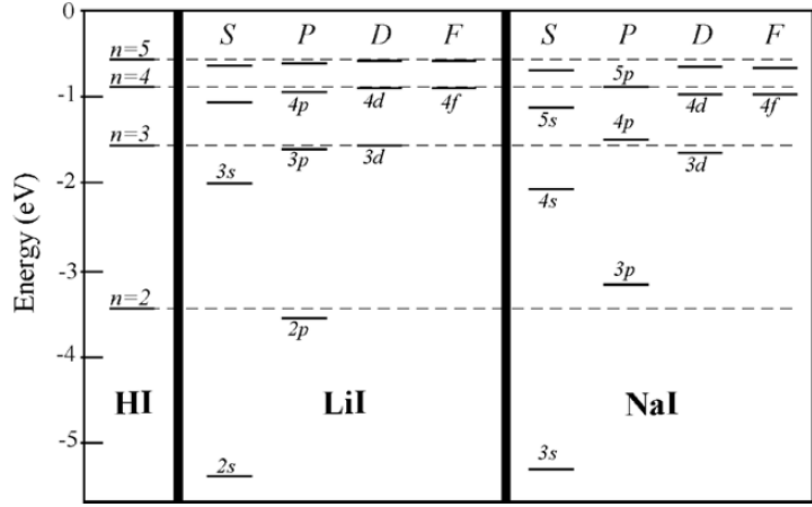
FIGURE 5.1: Energy-level diagrams of hydrogen, lithium, and sodium showing that the levels approximate those of hydrogen for high principal quantum numbers and high angular momentum quantum numbers. Figure taken from reference [33].

Property	n-scaling
$\langle r \rangle$	n^2
E_n	n^{-2}
τ (low-ℓ)	n^3
τ (high-ℓ)	n^5
ΔE_n	n^{-3}

Table 5.1: Scaling laws for properties of the Rydberg states: Orbital radius, state energy, radiative lifetime and separation between adjacent Rydberg levels.

Figure 5.2: Bohr orbits of $n = 1$ and $n = 10$. $a_0 = 0.53$ Å

system and the Rydberg constant

$$R^{(\infty)} = \frac{m_e}{4\pi\hbar^3} \left(\frac{e^2}{4\pi\epsilon_0} \right)^2 = \frac{Z^2\alpha^2 m_e c}{2\hbar} \qquad (5.2)$$

was related to the mass and charge of the electron. This in conjunction with the full quantum mechanical treatment from the Schrödinger equation allowed to find scaling laws for the atomic properties in terms of the principal and angular momentum quantum numbers n and ℓ, as listed in table 5.1.

At high n and ℓ, or Rydberg states, the valence electrons have binding energies which decrease as n^{-2} and orbital radii which increase as n^2. Therefore in a Rydberg atom, the valence electron is in a large, loosely bound orbit. For example, the ground state of H is bound by 1 Rydberg, 13.6 eV, and has an orbital radius of a_0. In contrast, the $n = 10$ state has a binding energy of $0.01R$ and orbital radius of $100a_0$, as shown in figure 5.2. The fact that this highly excited atomic states have no overlap with the nucleus makes Rydberg atoms an interesting platform to study any possible New Physics of long-range mediators free of the nuclear effects. Particularly, Rydberg states with the maximum angular momentum $\ell = n - 1$, so-called circular states because the probability density is significant only in an annular region centered on the nucleus, are of interest. Conveniently, such states have the longest lifetime in a given shell n and enjoy suppressed Stark effect. In fact, circular Rydberg states of hydrogen in the microwave regime have been used in very precise measurements of transition frequencies setting a value for the Rydberg constant with a 2.1×10^{-11} relative uncertainty [34, 35].

The empirical quantum defect factor δ_ℓ has to be experimentally determined for each single atom and its particular states. This factor in formula (5.1) encapsulates all the corrections to the experimental ionization values. It thus encodes all the complex dynamics hidden in the atoms that deviate from the simple Bohr atom physics. Apart from being a measure of the deviation from
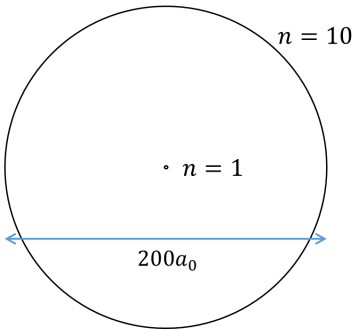
the Bohr atom, as depicted in figure 5.1 is, in fact, the quantum defect δ_ℓ is a measure of the phase shift of the wave function for the multielectron atom from that for a hydrogen atom. In this picture, the outermost or "valence" electron experiences a pure Coulomb potential when it is beyond some critical distance from the nucleus, but is "scattered" when it encounters the ionic core composed of the nucleus and the remaining electrons.

It is well-known that equation (5.1) fits particularly well the energy series of alkali-metal atoms, which have one electron outside a closed shell configuration. Thus, an alkali atom may be thought of as a "one-electron" atom, the electron residing in a potential provided by the nucleus and core electrons. This effective potential is described in detail in §2.1. A direct connection between the non-hydrogenic contribution given by the effective potential V_{CF} in equation (2.23) and the quantum defect can be established semi-classically as

$$\delta_\ell = -\frac{1}{2\pi} \int_{\text{orbit}} V_{\text{CF}}(r)\mathrm{d}t, \tag{5.3}$$

where the integration is performed over the classical orbit of the electron [33]. In this sense, by studying the effective potential one is able to essentially capture the full atom dynamics.

5.2 Bounding Linearity

As described in §4.2, the appearance of a new force carrier will lead to a linearity breaking in the polarization plot through (*i*) the NP electronic properties and (*ii*) the King's plot, as it will modify the isotopes shifts via the nuclear couplings of the NP.

Both approaches above can be used to bound the properties of the NP mediator. In the following, I describe how to make projections bounds using alkali Rydberg atoms.

5.2.1 Isotope Shifts for Rydberg states

As described in §3.2.1, the reduced IS of a transition $\wp$ is given by

$$(\Delta\nu_\wp)^{AA'} = K_\wp \mu_{AA'}^{-1} + F_\wp \lambda^{AA'}. \tag{5.4}$$

The two terms on the equation above represent the Specific Mass Shift (SMS) and the Field Shift (FS), respectively, where both μ_{AB} and λ_{AB} are purely nuclear quantities and are not dependent on the chosen electronic transition $\wp$. On the other hand, the parameters $K_\wp$ and $F_\wp$ are dependent on the transition $\wp$ but independent on the isotope, where

$$K_\wp = \langle \Psi_{\gamma,n\ell} | \sum_{i<j} \mathbf{p}_i \cdot \mathbf{p}_j | \Psi_{\gamma,n\ell} \rangle - \langle \Psi_{\gamma',n'\ell'} | \sum_{i<j} \mathbf{p}_i \cdot \mathbf{p}_j | \Psi_{\gamma',n'\ell'} \rangle \tag{5.5}$$

is an exchange factor due to the electron-electron polarization inside the atom [16] and to first order

$$F_a = (2\pi/3)Ze^2\left(|\Psi_{\gamma,n\ell}(0)|^2 - |\Psi_{\gamma',n'\ell'}(0)|^2\right) \qquad (5.6)$$

is an electronic factor proportional to the change in electron density at the nucleus between the initial and final electronic state [17]. In this way, each term above is a factorization of nuclear and electronic dependent quantities.

When Rydberg atoms are used to measure such IS, the specific contribution of the electronic and nuclear factors are easily understood. In Rydberg atoms, one can assume that the Rydberg electron is distinguishable from the electrons in the ion core as it is always farther away from the nucleus than any of the core electrons. In this sense, with atomic zeroth-order wavefunction $|\Psi_{\gamma,n\ell}^{(0)}\rangle = |\varphi_\gamma^{\text{core}}\rangle\,|\psi_{n\ell}^{\text{Ryd}}\rangle$ in equation (2.11) and assuming that the transition $\wp$ do not modify the quantum state of the core-electron wavefunction, the isotope shift factors will become independent of the Rydberg electron state and then the FS electronic factor will reduce to

$$F_\wp = (2\pi/3)Ze^2\left(|\varphi_{\gamma'}^{\text{core}}(0)|^2 - |\varphi_\gamma^{\text{core}}(0)|^2\right) = 0. \qquad (5.7)$$

The above can be seen as a consequence of diminished interaction of the Rydberg electron with the nucleus and core electrons and its close proximity to the ionization energy [36], where $|\psi_{n\ell}^{\text{Ryd}}(0)|^2$ the Rydberg electron electronic density at the nucleus is zero. The SMS factor will have a similar behavior, with

$$\begin{aligned} K_\wp =\ & \langle\varphi_\gamma^{\text{core}}|\sum_{i<j}\mathbf{p}_i\cdot\mathbf{p}_j|\varphi_\gamma^{\text{core}}\rangle \\ & - \langle\varphi_\gamma^{\text{core}}|\sum_{i<j}\mathbf{p}_i\cdot\mathbf{p}_j|\varphi_\gamma^{\text{core}}\rangle \approx 0, \qquad (5.8)\end{aligned}$$

where the approximations stands from the fact that higher-order correlation effects in the electronic wave-function might appear. Thus, if this correlation effects are important then a complete description of the SMS and the validity of the result above will require precise knowledge of the electronic wavefunctions. In that case, the IS in the King relation(4.7) is proportional only to the Mass Shift and any non-linearity can be related to deviations in μ^{AB}.

From the discussion above, one would be tempted to completely disregard the FS effects. However, wavefunctions of the core electrons are required to calculate the Rydberg electron effective potential, implying that any FS in the core wavefunction due to nuclear effects will translate into a isotope dependent modification of the effective potential parameters[17].

To see how the IS will behave for Rydberg atoms, consider again the transition $\wp \equiv n\ell \to n'\ell'$. The transition frequency $\nu_\wp{}^A$

[17] See equation (2.16) and the discussion around.

of an isotope A in first order in perturbation theory is

$$
2\pi\hbar\nu_\wp{}^A = -\frac{e^2}{(4\pi\epsilon_0)a_0}\frac{\mu_A}{m_e}\left(\frac{1}{2n'^2} - \frac{1}{2n^2}\right)
$$
$$
- \frac{\alpha_A^{E1}}{2}\left(\frac{\mu_A}{a_0 m_e}\right)^4\left\langle\frac{1}{r^4}\right\rangle_\wp - \frac{\alpha_A^{E2}}{2}\left(\frac{\mu_A}{a_0 m_e}\right)^6\left\langle\frac{1}{r^6}\right\rangle_\wp
$$

$$(5.9)$$

where the brackets indicate the expectation values with respect to the analytical Hydrogenic wavefunctions and $\langle r^{-\kappa}\rangle_\wp = \langle r^{-\kappa}\rangle_{n'\ell'} - \langle r^{-\kappa}\rangle_{n\ell}$.

The reduced[18] Isotope Shift $\nu_a{}^{AB}$ of the transition is then

$$
2\pi\hbar\nu_\wp{}^{AB} = \left[\sum_{k=1,2}\frac{\alpha_A^{Ek}}{2}\frac{1}{a_0^{2(k+1)}}\left\langle\frac{1}{r^{2(k+1)}}\right\rangle_\wp\right]\mu_{AB}
$$
$$
+ \sum_{k=1,2}\frac{(\Delta\alpha^{Ek})_{AB}}{2}\left(\frac{\mu}{a_0 m_e}\right)^{2(k+1)}\left\langle\frac{1}{r^{2(k+1)}}\right\rangle_\wp \quad (5.10)
$$

Here we see that the terms from the long-range polarization potential can be factorized. Together with the NMS and can also be reabsorbed in the electronic factor $K_\wp$, much in the sense of seeing this polarization effects as the responsible for the SMS. On the other hand, any possible second order nuclear effect on the model potential parameter is taken into account by the isotopic change of the polarizabilities $(\Delta\alpha^{Ek})_{AB} = \alpha_B^{Ek} - \alpha_A^{Ek}$. By using a semi-classical approach with the Thomas-Fermi-Dirac description of the atom, we can set a conservative bound on the isotopic change of the polarizability coefficients $(\Delta\alpha^{Ek})_{AB}/\alpha^{Ek} \sim 10^{-5}$, concluding that the second term in the right hand side of equation (5.10) is below of the order of the experimental precision[19]. In the left column of figure 5.4, the size of the isotopic change of the polarizability coefficients $\nu_{\Delta\alpha}$ in the King's plot linearity (5.10) compared with the transition frequency $\nu_\wp$, that is,

$$
\frac{\nu_{\Delta\alpha}}{\nu_\wp^A} \equiv \frac{1}{(2\pi\hbar)\nu_\wp^A}\sum_{k=1,2}\frac{(\Delta\alpha^{Ek})_{AB}}{2}\left(\frac{\mu}{a_0 m_e}\right)^{2(k+1)}\left\langle\frac{1}{r^{2(k+1)}}\right\rangle_\wp.
$$

$$(5.11)$$

is shown. One can see that the fractional contribution of $\nu_{\Delta\alpha}$ scales up with the number of electrons, which is directly related to the polarizabilities α^{Ek}, and scales down for transitions $\wp$ with higher quantum numbers. The ability to neglect this contributions relies on selecting the right atomic species and transition that will have a fractional contribution well below the experimental uncertainty.

Under this considerations, the IS of Rydberg states with no overlap with the nucleus or core electrons wavefunctions will have a the form

$$
2\pi\hbar\nu_\wp{}^{AB} = \widetilde{K}_\wp\mu_{AB}, \quad (5.12)
$$

with

$$\widetilde{K}_\wp \equiv \left[\sum_{k=1,2} \frac{\alpha_A^{Ek}}{2} \frac{1}{a_0^{2(k+1)}} \left\langle \frac{1}{r^{2(k+1)}} \right\rangle_\wp \right] \quad (5.13)$$

being the electronic factor accompanying the reduced mass term. Hence, one is able to bound non-linearities on the IS just by tracking the linear behavior of a defined transition frequency $\nu_\wp$ in terms of the reduced mass difference μ_{AB}.

Here lays the power of the method of using Rydberg states. The number of required transitions is reduced to one, no complex calculation of multi-electron factors is required, and nuclear factors drop completely from the linearity formula. The price one pays is much reduced ability to bound heavy NP mediators with the relevant masses being

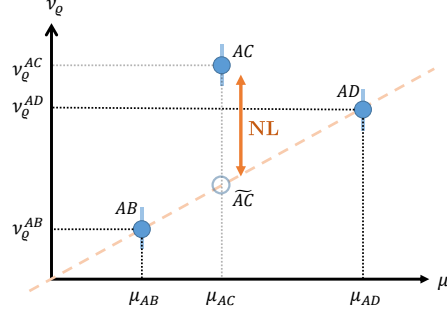$$m_\phi^{\mathrm{exp}} = \hbar / r_{\mathrm{exp}} c = m_e \alpha \ell^{-2}. \quad (5.14)$$

5.2.2   Tracing non-linearities

Consider now the presence of a new force carrier that couples electrons and neutrons. The IS formula (5.12) is modified as

$$2\pi\hbar\nu_\wp{}^{AB} = \widetilde{K}_\wp \mu_{AB} + \alpha_{\mathrm{NP}} X_\wp \gamma_{AA'}, \quad (5.15)$$

as described in §4.2.2. To trace the existence of non-linearity, consider the IS of pairs of isotopes (AB, AC, AD), giving three points in the figure 5.3. If we take an hypothetical point $\widetilde{AC}$ lying in the line formed by the points AB and AD determined by equation (5.12), the non-linearity of the point AC given by (5.15) can be defined as

$$\mathrm{NL} \equiv (\widetilde{AC} - AC) = (2\pi\hbar)^{-1} \alpha_{\mathrm{NP}} X_\wp \gamma_{AA'}. \quad (5.16)$$

In that way, an experiment with some accuracy σ on the determination of the values is able to bound linearity if NL is lower than the experimental accuracy. Qualitatively, a given set of data is linear if

$$\mathrm{NL} \lesssim \sigma_{\mathrm{NL}} = \sqrt{\sum_k (\partial \mathrm{NL}/\partial O_k)^2 \sigma_k^2} \quad (5.17)$$

where σ_{NL} is the first-order propagated error due to the errors in the experimental parameter O_k with standard deviations σ_k.

The proposed measure of non-linearity NL is in units of frequency. It is possible then to estimate the possible bounds that can be set on a new mediator given that the fractional contribution of NL to the IS in equation (5.16) is below the relative experimental uncertainty. The right column of figure 5.4 shows the projected bounds on the coupling $y_e y_n$ of a new force mediator given some experimental precision. It is possible to see how the ability to bound heavier mediators decreases for heavier atoms.

Figure 5.3: Schematic illustration of the nonlinearity NL. The IS frequencies $\nu_\wp$ and $\nu_\wp{}^{AD}$ are plotted for the three pairs of isotopes (AB, AC, AD) in solid blue circles. The line joining the points AB and AC has slope $\widetilde{K}_\wp$. The difference between point AC and the hypothetical point lying on the same line $\widetilde{AC}$ (open blue circle) as AB and AD leads to the evaluation of nonlinearity of equation (5.15). The bars accompanying the dots represent the error bars or accuracy of the experimental value.
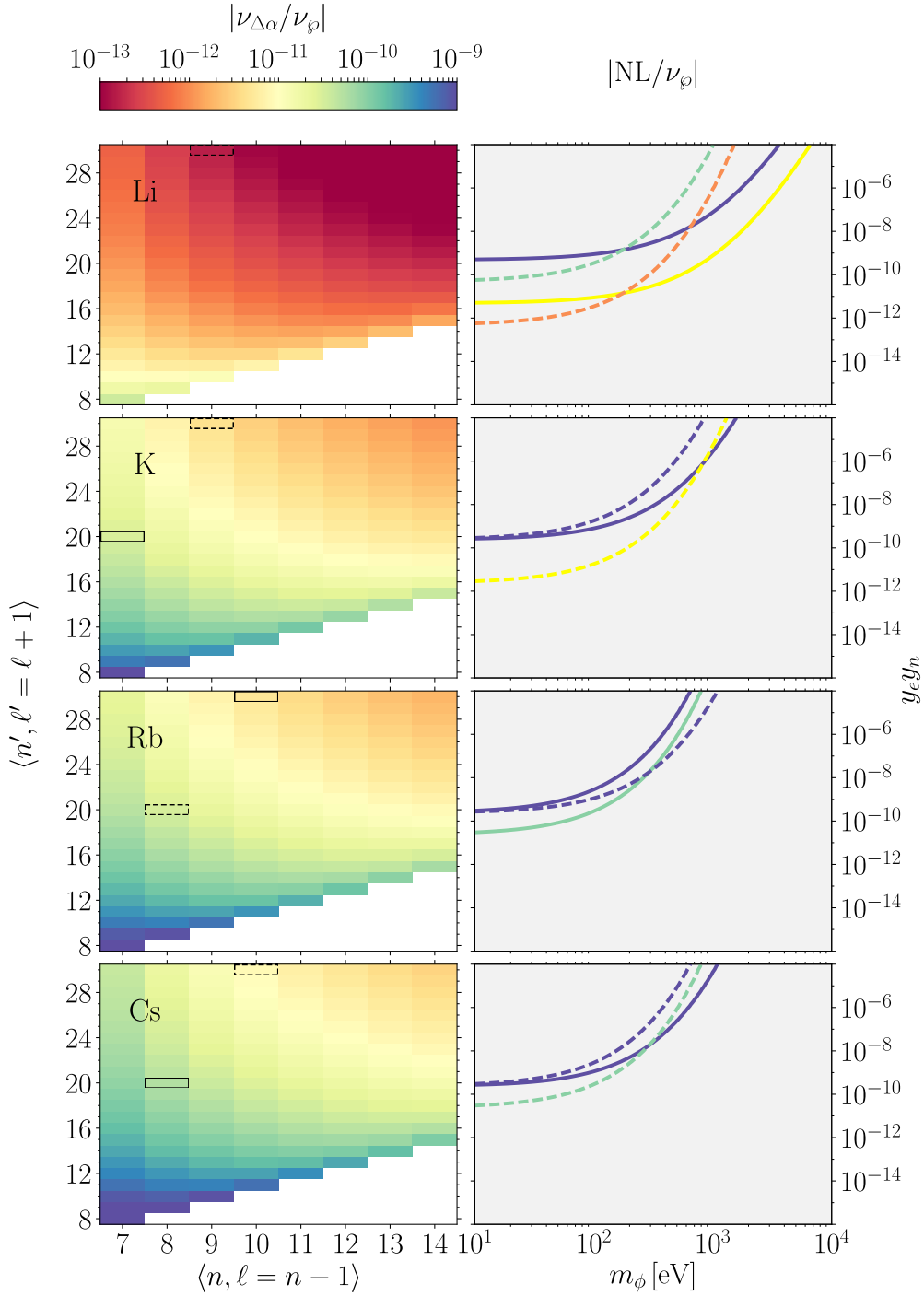
FIGURE 5.4

FIGURE 5.5: **Left column:** fractional size of the isotopic change of the polarizability coefficients $\nu_{\Delta\alpha}$ (indicated in the color bar) as defined in equation (5.11), for the transitions $\wp = n\ell \to n'\ell'$ from the initial circular states $\ell = n - 1$ (indicated in the horizontal and vertical labels). The dashed- and solid-line boxes show the transitions used in the right column. **Right column:** Projected bounds on the coupling $y_e y_n$ of a new force mediator of mass m_ϕ for the experimental fractional accuracy indicated by the line color (and its respective value in the color bar). Solid and dashed lines correspond to the boxed transitions in the left column, respectively.

To understand this better, lets consider three regions for the interaction range of the NP potential $V_{\mathrm{NP}}(r; m_\phi) = \alpha_{\mathrm{NP}} e^{-r/\lambda_\phi}/r$ set by the mediator mass m_ϕ.

- In the massless limit $m_\phi < m_{\mathrm{exp}}$ where the interaction range is larger than the atomic size, the NP potential behaves as $V_{\mathrm{NP}} \to \alpha_{\mathrm{NP}}/r$, that is, the NP is independent on the mass and any non-linearity can be related to deviations of the transition frequency due to the modified Coulomb potential of the electron.

- For masses $m_\phi \sim m_{\mathrm{exp}}$ that have comparable Compton wavelength with the size of the electron orbit, the interaction range is within the electron wavefunction and the potential is mass dependent $V_{\mathrm{NP}} \to \alpha_{\mathrm{NP}} e^{-r/\lambda_\phi}/r$. In this region, where the Rydberg electron is more sensitive to the NP mediator, one is able to bound both the coupling and mass of the new particle.

- In the heavy mass limit $m_\phi < m_{\mathrm{exp}}$ the sensitivity of the Rydberg electron to the NP mediator is lost and thus the bounds rapidly diverge.

As shown in figure 5.4, different atomic species will have different sensitivity to NP. This is determined by the size of the electronic core that condition the model potential approximation for states with higher angular momentum . Higher angular momentum in turn implies reduced sensitivity as it scales like $m_\phi^{\mathrm{exp}} = \hbar/r_{\mathrm{exp}}c = m_e \alpha \ell^{-2}$. One is then required to wisely choose an electronic transition that on one hand reduces the electronic effects of the isotopic change of the model potential parameters, but on the other hand stay in the relevant regime where the electron is in the range of the NP mediator.

A data-driven bound is currently unavailable as the transitions of interest are experimentally not explored or the more studied elements have not enough stable isotopes that can be used to perform experimental measurements. A few elements, like Cesium, Rubidium, Potassium and Lithium, do have unstable isotopes with long lifetimes that can potentially open an avenue for the required measurements. Still, manipulation of unstable isotopes is generally complicated. This motivates a future complementary approach, described in Appendix C, where the electronic properties of the NP are exploited intead of the isotopic change.

Alkali Rydberg atoms are shown to be good probes for the search of new low-mass mediators where nuclear and multi-electronic effects that could be confused with the new physics signal can be traced out, as discussed throughout this section. In the following section the results and future directions of this work are summarized, the best projected Rydberg bounds on NP are shown and compared with existing experimental data.

Chapter 6

Projected Bounds and Concluding Remarks

In this thesis a strategy to formulate a set of observables that are sensitive to the presence of new mass-dependent NP force mediators in Rydberg atoms was elaborated. Rydberg atoms are independent to leading order of nuclear effects, and thus the observables developed require less transitions than the King's plot approach.

To this end, we studied the effective model potential that describes the interaction of the Rydberg electron with the charge distribution of the core electrons, avoiding in that way the complicated and computer-expensive many-body relativistic core electronic wavefunction calculations. I turn, we rely on available compiled data for the elements of interest.

However, the precision to which the parameters of the model potential are known is limited. It is thus necessary to find atomic transition lines in which the magnitude of the effects that deviate from the Coulomb-like interactions are lower than the expected experimental precision. This sets the range to which NP can be bound by the system; atomic states with high quantum number and large orbital radius enjoy suppressed non-Coulomb effects but suffer from reduced ability to couple to heavy-mass NP mediators. One needs to find a balance between the devil of the reduced ability to bound and the deep blue sea of having to deal with complicated many-body core-electron effects. Once precision calculations for the model potential parameters become available, where the uncertainty for their values is below order unity, the ability of our method will be much improved. Even thought this strongly encourages numerical calculations of the model potential parameters, they were out of the scope of this thesis.

We show that, to first order, the dynamics of the Rydberg levels is free from nuclear structure effects and that all the isotope-shifts involving Rydberg transitions scale as the Normal Mass Shift (NMS). As a consequence, a linear relation between the reduced mass difference $\mu_{AA'} = \mu_{A'} - \mu_A$ of an isotopic sequence and the isotope-shift of a selected transition $\wp$ can be found,

$$\nu_\wp^A - \nu_\wp^{A'} = K_\wp \mu_{AA'}. \tag{6.1}$$

Due to this linear behavior and as opposed to King's plot linearity approach, one can bound NP with the need of less isotopes and only one transition, a feature that is advantageous for the atomic systems of interest.

Second order nuclear structure effects enter into the parameters of the model potential and can break the linearity described above. For this reason it becomes important to estimate the order of these effects. A full description of them requires knowledge of the many-body wavefunctions of the electronic core and, as these calculations are in general not available, a semi-classical approach is used to calculate the isotopic variability of the model potential parameters by using the Thomas-Fermi description of the atom. Within this model, it is found that any second-order nuclear size effect on the model potential will be well below the experimental precision and then can be safely disregarded.

The projected bounds for several atomic states in different Alkali metal atoms were calculated by scanning the parameter space of the NP mediator to find the Rydberg levels with the most suppression of electronic effects and the highest ability to bound NP. In figure 6.1 the best projected bounds for the atomic species studied are compared with experimental data for Calcium and existing constraints from other experiments [2].

As a conclusion, using Rydberg transitions in one valence electron atomic systems, we formulated a complementary observable to the King's plot able to bound NP mediators using high-precision measurements. The power of the method relies on the decoupling of the nuclear effects and many-body core electron effects from the dynamics of the Rydberg electron, allowing for a reformulated mass-to-frequency linearity. Contrary to the King's plot, this approach requires with less transitions and potentially atomic systems with less isotopes. This would enable more atomic systems to be used as low-energy probes for NP in order to bound low-mass NP mediators with a precision comparable to other astrophysical approaches and even possibly setting the strongest atomic-based bound. For mid- to high-mass mediators, the method does not provide good bounds as the sensitivity is heavily reduced due to the decreased coupling of the Rydberg electron with the NP mediator.
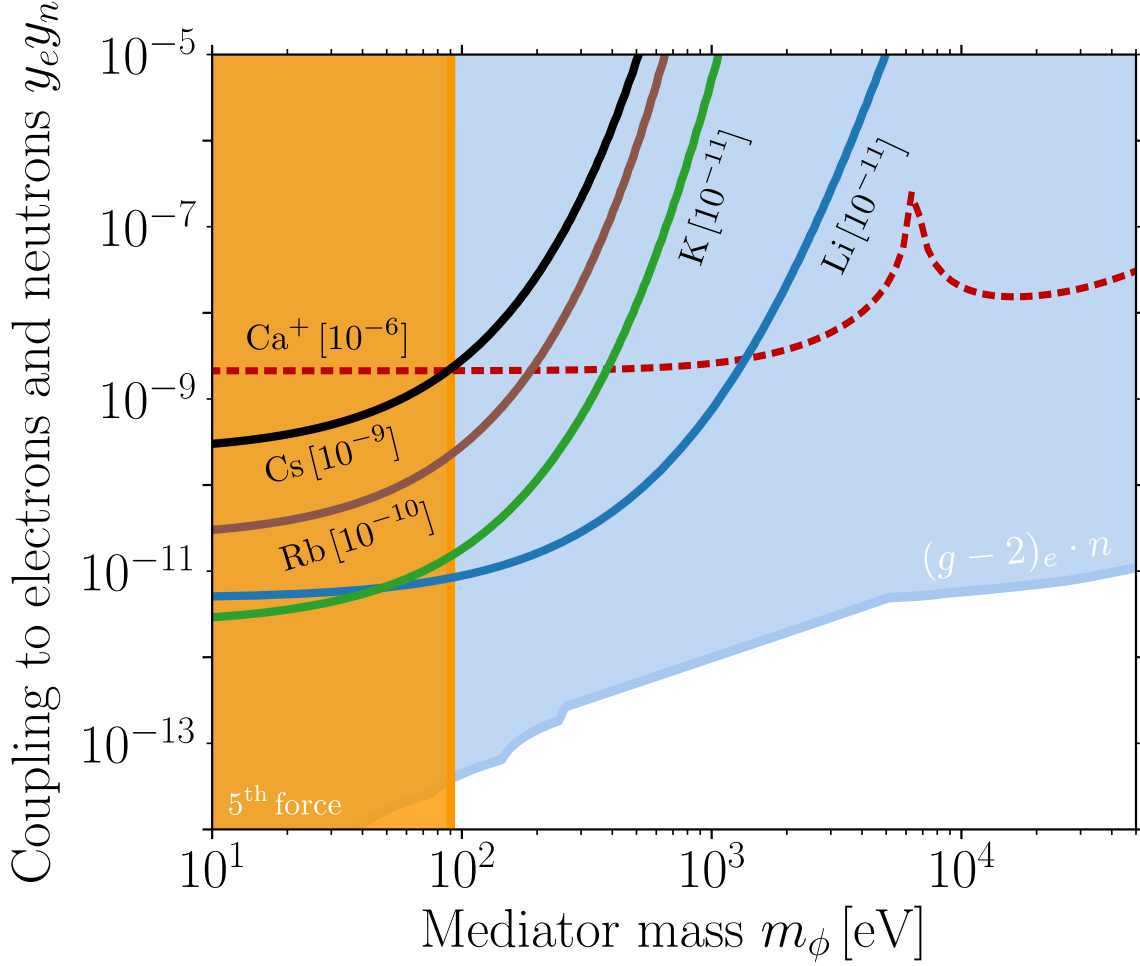
FIGURE 6.1: Limits on the electron and neutron couplings $y_e y_n$ of a new boson of mass m_ϕ for the fractional experimental accuracies σ specified on the square brackets. Existing constraints from Ca^+ IS are shown in the dahed red line, existing constraints from other experiments are shown as shaded areas: fifth force (dark orange) $(g-2)_e$ combined with neutron scattering (light blue) [2]. Best projected bounds using Rydberg states (this work) for the alkali atoms labeled are shown in solid lines.

"(Uno se embarca hacia tierras lejanas, o busca el conocimiento de hombres, o indaga la naturaleza, o busca a Dios; despue advierte que el fantasma que se persegura Uno mismo.)"

—*Uno y el Universo*, Ernesto Sabato.

"(One embarks towards distant lands, or looks for the knowledge of men, or inquires about nature, or seeks God; then one notices that the ghost that one went after is Oneself.)" _{*(free translation)}

—*One and the Universe*, Ernesto Sabato.

Appendix A

Center of Mass frame

Consider the non-relativistic Hamiltonian of an atom with N electrons of mass m_e located at positions $\mathbf{r}_i$ for $i = 1, \ldots, N$ and a nucleus of mass $m_A = Z m_p + (A - Z) m_n$ at $\mathbf{r}_0$,

$$H = \frac{p_0^2}{2 m_A} + \sum_{i=1}^{N} \frac{p_i^2}{2 m_e} + \sum_{i=1}^{N} V_{eN}(\mathbf{r}_i - \mathbf{r}_0) + \frac{1}{2} \sum_{i \neq j} V_{ee}(\mathbf{r}_i - \mathbf{r}_j), \quad (A.1)$$

where $V_{eN}(\mathbf{r}_i - \mathbf{r}_0)$ is the Coulomb potential between i–th electron with the nucleus and $V_{ee}(\mathbf{r}_i - \mathbf{r}_j)$ the Coulomb potential between electrons. The dynamics are best described in the center of mass (CM) coordinate

$$\mathbf{R}_{CM} = \frac{m_A \mathbf{r}_0 + m_e \sum_{i=1}^{N} \mathbf{r}_i}{M} \quad (A.2)$$

and the difference coordinate $\boldsymbol{\rho}_i = \mathbf{r}_i - \mathbf{r}_0$ of the complete system. The generalised momenta of this coordinate system is $\mathbf{P}_{CM} = -\hbar \boldsymbol{\nabla}_R$ and $\boldsymbol{\pi}_i = -\hbar \boldsymbol{\nabla}_{\rho_i}$, respectively. With the above relations the old momentum can be rewritten in terms of the CM momentum as

$$\mathbf{p}_i = \boldsymbol{\pi}_i + \frac{m_e}{M} \mathbf{P}_{CM}, \quad \mathbf{p}_0 = -\sum_{i=1}^{N} \boldsymbol{\pi}_i + \frac{m_A}{M} \mathbf{P}_{CM}, \quad (A.3)$$

with $M = m_A + N m_e$ the total mass of the system.

Thus, the Hamiltonian in the CM coordinates is

$$H = \frac{1}{2M} P_{CM}^2 + \frac{1}{2\mu} \sum_{i=1}^{N} \pi_i^2 + \frac{1}{m_A} \sum_{i \neq j} \boldsymbol{\pi}_i \cdot \boldsymbol{\pi}_j$$

$$+ \sum_{i=1}^{N} V_{eN}(\boldsymbol{\rho}_i) + \frac{1}{2} \sum_{i \neq j} V_{ee}(\boldsymbol{\rho}_i - \boldsymbol{\rho}_j), \quad (A.4)$$

where $\mu^{-1} = m_A^{-1} + m_e^{-1}$ [5]. In this coordinates the dynamics of the CM is separated from the dynamics of the nucleus and the N electrons.

Appendix B

Static dipole polarizability in the Thomas-Fermi-Dirac model

The work related to this appendix was done together with Yogev Shpilman.

Here I describe the calculations were the method described in [37] to derive the static dipole polarizability of atoms and ions in the Thomas-Fermi-Dirac (TFD) model was followed. For extensive explanation of the TFD model see [38]. All the numerical calculations were done by Yogev and are described elsewhere.

The energy functional in the TFD is $E[\rho] = E_k + E_p + E_a$ where E_a is the exchange term. Applying variations $\delta E[\gamma]$ we get

$$(V - V_0)e - \frac{5}{3}x_\kappa\rho^{2/3} + \frac{4}{3}x_a\rho^{1/3} = 0, \tag{B.1}$$

such that the relation between the potential and the electron density is

$$\rho = \sigma_0\left[(V - V_0 + \tau_0^2)^{1/2} + \tau_0\right]^3 \tag{B.2}$$

with $\sigma_0 = (3e/5x_\kappa)^{3/2}$ and $\tau_0 = (4x_a^2/15x_k e)^{1/2}$.

The Laplace equation for the potential is

$$\nabla^2(V - V_0 + \tau_0^2) = 4\pi\sigma_0 e\left[(V - V_0 + \tau_0^2)^{1/2} + \tau_0\right]^3. \tag{B.3}$$

Let's assume now that there is a perturbation V' to the potential $V \to V + V'$ such that $V/V' \ll 1$ the equation above becomes

$$\nabla^2(V + V' - V_0 + \tau_0^2) = 4\pi\sigma_0 e\left[(V + V' - V_0 + \tau_0^2)^{1/2} + \tau_0\right]^3$$

$$\nabla^2(V - V_0 + \tau_0^2) + \nabla^2 V' \approx 4\pi\sigma_0 e\left\{\left[(V - V_0 + \tau_0^2)^{1/2} + \tau_0\right]^3\right.$$

$$\left.+ \frac{3}{2}\frac{\left[(V - V_0 + \tau_0^2)^{1/2} + \tau_0\right]^2}{(V - V_0 + \tau_0^2)^{1/2}}V' + \cdots\right\}$$

$$\nabla^2 V' \approx 4\pi\sigma_0 e\frac{3}{2}\frac{\left[(V - V_0 + \tau_0^2)^{1/2} + \tau_0\right]^2}{(V - V_0 + \tau_0^2)^{1/2}}V'$$

$$\tag{B.4}$$

where I used (B.3) for the last line. Assuming the potential $V' = (\mathbf{E} \cdot \mathbf{r})u(r) = Eru(r)\cos\theta$ with $\theta = \widehat{\mathbf{E}\mathbf{r}}$, then the above becomes

$$\frac{E\cos\theta}{r}\frac{\partial^2}{\partial r^2}\left(r^2 u(r)\right) + \frac{1}{r^2\sin\theta}\frac{\partial}{\partial\theta}\left(\sin\theta\frac{\partial}{\partial\theta}\left(Eru(r)\cos\theta\right)\right)$$
$$= 4\pi\sigma_0 e\frac{3}{2}\frac{\left[(V - V_0 + \tau_0^2)^{1/2} + \tau_0\right]^2}{(V - V_0 + \tau_0^2)^{1/2}}\left(Eru(r)\cos\theta\right)$$

$$\frac{\mathrm{d}^2 u}{\mathrm{d}r^2} + \frac{4}{r}\frac{\mathrm{d}u}{\mathrm{d}r} - 4\pi\sigma_0 e\frac{3}{2}\frac{\left[(V - V_0 + \tau_0^2)^{1/2} + \tau_0\right]^2}{(V - V_0 + \tau_0^2)^{1/2}}u = 0. \quad \text{(B.5)}$$

Applying the change of variables $r = bx$ and $\psi(x) = \frac{bx}{Ze}(V - V_0 + \tau_0^2)$

$$\frac{\mathrm{d}^2 u}{\mathrm{d}x^2} + \frac{4}{r}\frac{\mathrm{d}u}{\mathrm{d}x} - 4\pi\sigma_0 eb^2\frac{3}{2}\left(\frac{Ze}{b}\right)^{1/2}\left[\left(\frac{\psi}{x}\right)^{1/2} + \beta_0\right]^2\left(\frac{\psi}{x}\right)^{-1/2}u = 0, \quad \text{(B.6)}$$

with $\beta_0 = \tau_0\sqrt{\mu/Ze}$ and choosing b such that $4\pi\sigma_0 eb^{3/2}(Ze)^{1/2} = 1$

$$\frac{\mathrm{d}^2 u}{\mathrm{d}x^2} + \frac{4}{x}\frac{\mathrm{d}u}{\mathrm{d}x} - \frac{3}{2}\left[\left(\frac{\psi}{x}\right)^{1/2} + \beta_0\right]^2\left(\frac{\psi}{x}\right)^{-1/2}u = 0. \quad \text{(B.7)}$$

Setting $\beta = 0$ the expression above coincides with eqn. (14) in the paper.

With the boundary condition $\psi(0) = 1$ we can find a power-series solution to the differential equation around the point $x = 0$. So, if we change variables to $\xi = \sqrt{x}$, then

$$u(\xi) = \sum_{i=0}^{\infty} a_i\xi^i \quad \text{and} \quad \xi\frac{\mathrm{d}^2 u}{\mathrm{d}\xi^2} + 7\frac{\mathrm{d}u}{\mathrm{d}\xi} - 6\xi^2(1 + \xi\beta_0)^2 u = 0 \quad \text{(B.8)}$$

and one finds

$$u(x) = a_0\left(1 + \frac{2}{9}x^{3/2} + \cdots\right) \quad \text{such that} \quad \frac{\mathrm{d}u}{\mathrm{d}x}\bigg|_{x\to 0} = \frac{a_0}{3}x^{1/2}. \quad \text{(B.9)}$$

Because at the end we care about the ratio $u'(x)/u(x)$ the constant a_0 can be set to one.

With the above and the boundary conditions for $u(x)$ around x_0 then

$$\alpha = b^3 x_0^3\left[1 + \frac{3u(x_0)}{u'(x_0)}\right]^{-1}. \quad \text{(B.10)}$$

Appendix C

IS-enhanced Polarization plot

For the reasons exposed in the main text, a complementary approach is required where one can use less (stable) isotopes in the expense of more transitions. However, this approach has not been yet explored and then is not added to the main body of the thesis.

By looking closely again to the IS in equation (5.12), one realizes that the electronic factors are no other than the polarizabilities[20]. Then, instead of relying solely on the isotope behavior of the new force, one can find an observable that will exploit both the coupling to the nucleons as well as the electronic properties of the force.

In such a case, consider now *only* two isotopes A and B of the same atomic species and several transitions within the same or very close n and several ℓ quantum numbers. Then one can turn the IS formula (5.15) into an IS-enhanced polarization plot. Similarly to the polarization plot in §3.1, we can write

$$2\pi\hbar \frac{\nu_\wp{}^{AB}}{\langle r^{-4}\rangle_\wp} = \left[\frac{\alpha_A^{E1}}{2a_0^4} + \frac{\alpha_A^{E2}}{2a_0^6}\frac{\langle r^{-6}\rangle_\wp}{\langle r^{-4}\rangle_\wp}\right]\mu_{AB} + \alpha_{\mathrm{NP}}\frac{X_\wp}{\langle r^{-4}\rangle_\wp}\gamma_{AB}. \quad \text{(C.1)}$$

Here one would track linearity between

$$2\pi\hbar\frac{\nu_\wp{}^{AB}}{\langle r^{-4}\rangle_\wp} \quad \text{and} \quad \frac{\langle r^{-6}\rangle_\wp}{\langle r^{-4}\rangle_\wp}, \quad \text{(C.2)}$$

but the polarization factors defining the slope and the intercept of the linear plot will be weighted by μ_{AB}, reducing their absolute value a couple of orders of magnitude and hence becoming more sensitive to the NP term. Moreover, the mathematical behavior of the ratio $X_\wp/\langle r^{-4}\rangle$ is very distinct from the other terms in the expression above as

$$\alpha_{\mathrm{NP}}\frac{X_\wp}{\langle r^{-4}\rangle_\wp}\gamma_{AB} = -\gamma_{AB}\frac{\alpha_{\mathrm{NP}}}{\lambda_\phi}\frac{1}{\langle r^{-4}\rangle_\wp}$$

$$+ \gamma_{AB}\alpha_{\mathrm{NP}}\frac{\langle r^{-1}\rangle_\wp}{\langle r^{-4}\rangle_\wp} + \gamma_{AB}\alpha_{\mathrm{NP}}\sum_{n=1}^{\infty}\frac{1}{\lambda_\phi^{n+1}}\frac{\langle r^n\rangle_\wp}{(n+1)!}. \quad \text{(C.3)}$$

[20] In the leading order approach. Higher order terms will be also factorisable with μ_{AB} and thus they don't pose any problem for this approach.

The first term on the left hand side can be interpreted as a direct shift of the IS in (C.1)

$$2\pi\hbar \frac{\nu_\wp{}^{AB}}{\langle r^{-4}\rangle_\wp} \to 2\pi\hbar \frac{1}{\langle r^{-4}\rangle_\wp}\left(\nu_\wp{}^{AB} + \gamma_{AB}\frac{\alpha_{\mathrm{NP}}}{\lambda_\phi}\right), \qquad (C.4)$$

the second as a renormalization of the coupling constant α_{NP} to the Rydberg constant, and the third is a term with polynomial behavior that is very distinct from the others.

Bibliography

1. Safronova, M. *et al.* Search for new physics with atoms and molecules. *Reviews of Modern Physics* **90.** doi:`10.1103/revmodphys.90.025008` (2018).

2. Berengut, J. C. *et al.* Probing New Long-Range Interactions by Isotope Shift Spectroscopy. *Physical Review Letters* **120.** doi:`10.1103/physrevlett.120.091801` (2018).

3. Flambaum, V. V., Geddes, A. J. & Viatkina, A. V. Isotope shift, nonlinearity of King plots, and the search for new particles. *Physical Review A* **97.** doi:`10.1103/physreva.97.032510` (2018).

4. Hughes, D. S. & Eckart, C. The Effect of the Motion of the Nucleus on the Spectra of Li I and Li II. *Phys. Rev.* **36,** 694–698 (4 1930).

5. Johnson, W. R. *Many-Body Calculations of the Isotope Shift* `https://www3.nd.edu/~johnson/Publications/i_shift.pdf`. Mar. 2011. <`https://www3.nd.edu/~johnson/Publications/i_shift.pdf`>.

6. Bransden, B. & Joachain, C. *Physics of Atoms and Molecules* ISBN: 9780582356924. <`https://books.google.co.il/books?id=i5IPWXDQlcIC`> (Prentice Hall, 2003).

7. Mitroy, J, Safronova, M. S. & Clark, C. W. Theory and applications of atomic and ionic polarizabilities. *Journal of Physics B: Atomic, Molecular and Optical Physics* **43,** 202001 (2010).

8. Woods, S. L. & Lundeen, S. R. Effective-potential model for high-L Rydberg atoms. *Physical Review A* **85.** doi:`10.1103/physreva.85.042505` (2012).

9. Lundeen, S. R. in *Advances In Atomic, Molecular, and Optical Physics* 161–208 (Elsevier, 2005). doi:`10.1016/s1049-250x(05)52004-4`.

10. Peach, G. in *Atoms in Astrophysics* (eds Burke, P. G., Eissner, W. B., Hummer, D. G. & Percival, I. C.) 115–171 (Springer US, Boston, MA, 1983). ISBN: 978-1-4613-3536-8. doi:`10.1007/978-1-4613-3536-8_5`. <`https://doi.org/10.1007/978-1-4613-3536-8_5`>.

11. Laughlin, C. On the accuracy of the Coulomb approximation and a model-potential method for atomic transition probabilities in alkali-like systems. *Physica Scripta* **45,** 238 (1992).

12. Theodosiou, C. E. Evaluation of penetration effects in high-*l* Rydberg states. *Phys. Rev. A* **28,** 3098–3101 (5 1983).

13.   Marinescu, M., Sadeghpour, H. R. & Dalgarno, A. Dispersion coefficients for alkali-metal dimers. *Phys. Rev. A* **49,** 982–988 (2 1994).

14.   Šibalić, N., Pritchard, J., Adams, C. & Weatherill, K. ARC: An open-source library for calculating properties of alkali Rydberg atoms. *Computer Physics Communications* **220,** 319–331 (2017).

15.   Delaunay, C., Ozeri, R., Perez, G. & Soreq, Y. Probing atomic Higgs-like forces at the precision frontier. *Physical Review D* **96.** doi:`10.1103/physrevd.96.093001` (2017).

16.   Sobel'man, I. *Introduction to the Theory of Atomic Spectra* <`https://books.google.co.il/books?id=TFc7vgAACAAJ`> (Pergamon Press, 1972).

17.   Drake, G. *Springer Handbook of Atomic, Molecular, and Optical Physics* ISBN: 9780387263083. <`https://books.google.co.il/books?id=Jj-ad\_2aNOAC`> (Springer, 2006).

18.   Pálffy, A. Nuclear effects in atomic transitions. *Contemporary Physics* **51.** See Section IIB, 471–496 (2010).

19.   Mitroy, J. & Safronova, M. S. Polarizabilities of the Mg^+ and Si^{3+} ions. *Physical Review A* **79.** doi:`10.1103/physreva.79.012513` (2009).

20.   Booth, D. W., Isaacs, J. & Saffman, M. Reducing the sensitivity of Rydberg atoms to dc electric fields using two-frequency ac field dressing. *Physical Review A* **97.** doi:`10.1103/physreva.97.012515` (2018).

21.   Mohr, P. J., Newell, D. B. & Taylor, B. N. CODATA recommended values of the fundamental physical constants: 2014. *Reviews of Modern Physics* **88.** doi:`10.1103/revmodphys.88.035009` (2016).

22.   Fricke, G. *et al.* Nuclear Ground State Charge Radii from Electromagnetic Interactions. *Atomic Data and Nuclear Data Tables* **60,** 177–285 (1995).

23.   King, W. H. Comments on the Article "Peculiarities of the Isotope Shift in the Samarium Spectrum". *J. Opt. Soc. Am.* **53,** 638–639 (1963).

24.   King, W. H. *Isotope Shifts in Atomic Spectra* doi:`10.1007/978-1-4899-1786-7` (Springer US, 1984).

25.   Budker, D. *Atomic physics: an exploration through problems and solutions* eng. ISBN: 0198509502 (Oxford University Press, Oxford, 2004).

26.   Dobrescu, B. A. & Mocioiu, I. Spin-dependent macroscopic forces from new particle exchange. *Journal of High Energy Physics* **2006,** 005–005 (2006).

27.   Thomson, M. *Modern Particle Physics* 570 pp. ISBN: 1107034264. <`https://www.ebook.de/de/product/20673687/mark_thomson_modern_particle_physics.html`> (Cambridge University Pr., Sept. 5, 2013).

28. Snow, E. L. & Lundeen, S. R. Determination of dipole and quadrupole polarizabilities ofMgby fine-structure measurements in high-Ln=17Rydberg states of magnesium. *Physical Review A* **77.** doi:`10.1103/physreva.77.052501` (2008).

29. Ward, R. F., Sturrus, W. G. & Lundeen, S. R. Microwave spectroscopy of high-LRydberg states of neon. *Physical Review A* **53,** 113–121 (1996).

30. Hanni, M. E., Keele, J. A., Lundeen, S. R. & Sturrus, W. G. Microwave spectroscopy of high-Ln=10Rydberg states of argon. *Physical Review A* **78.** doi:`10.1103/physreva.78.062510` (2008).

31. Gallagher, T. F. *Rydberg Atoms (Cambridge Monographs on Atomic, Molecular and Chemical Physics)* ISBN: 0-521-38531-8. <`https://www.amazon.com/Rydberg-Cambridge-Monographs-Molecular-Chemical/dp/0521385318?SubscriptionId=0JYN1NVW651KCA56C102&tag=techkie-20&linkCode=xm2&camp=2025&creative=165953&creativeASIN=0521385318`> (Cambridge University Press, 1994).

32. Pohl, R. *et al.* The size of the proton. *Nature* **466,** 213–216 (2010).

33. Charles E. Burkhardt, J. J. L. *Topics in Atomic Physics* ISBN: 0387257489. <`https://www.ebook.de/de/product/4291683/charles_e_burkhardt_jacob_j_leventhal_topics_in_atomic_physics.html`> (Springer-Verlag GmbH, Nov. 16, 2005).

34. De Vries, J. C. *A precision millimeter-wave measurement of the Rydberg frequency* PhD thesis (Massachusetts Institute of Technology, Jan. 2001).

35. Ramos, A., Moore, K. & Raithel, G. Measuring the Rydberg constant using circular Rydberg atoms in an intensity-modulated optical lattice. *Physical Review A* **96.** doi:`10.1103/physreva.96.032513` (Sept. 2017).

36. Aldridge, L., Gould, P. L. & Eyler, E. E. Experimental isotope shifts of the 5 2S1/2state and low-lying excited states of Rb. *Physical Review A* **84.** doi:`10.1103/physreva.84.034501` (2011).

37. Shevelko, V. P. & Vinogradov, A. V. Static Dipole Polarizability of Atoms and Ions in the Thomas-Fermi Model. *Physica Scripta* **19,** 275–282 (1979).

38. Gombas, P. *Die Statistische Theorie des Atoms und ihre Anwendungen* ISBN: 3709121019. <`https://www.ebook.de/de/product/22335622/pal_gombas_die_statistische_theorie_des_atoms_und_ihre_anwendungen.html`> (Springer-Verlag KG, Apr. 18, 2014).